Please cite this article as:

Bombrys M., Matysiak K., Kardasz P. 2026. Interaction of spatial planting arrangement and plant density on intraspecific competition in two maize cultivars. Journal of Plant Protection Research. DOI: 10.24425/jppr.2026.3649

Original article

Interaction of spatial planting arrangement and plant density on intraspecific competition in two maize cultivars

Marcin Bombrys[1], Kinga Matysiak[2], Przemysław Kardasz[1]

[1] Field Experimental Station in Winna Gora, Institute of Plant Protection - National Research Institute, Poznan, Poland
[2] Department of Weed Sciences and Plant Protection Technique, Institute of Plant Protection - National Research Institute, Poznan, Poland

*Corresponding address: k.matysiak@iorpib.poznan.pl

Received: May 20, 2026

Accepted: August 20, 2026

Online Pree-Proof Publication: September 7, 2026

Responsible Editor: Jolanta Kowalska

DOI: 10.24425/jppr.2026.3649

Abstract

A three-year field study was carried out to assess the intraspecific competitiveness of selected maize (*Zea mays* L.) cultivars under different plant densities and spatial arrangements during the growing season. The central hypothesis posited that plant spacing, population density per unit area, and cultivar type significantly influence maize morphology and yield performance. Furthermore, these factors were expected to affect growth dynamics and the level of competition between individual plants within the same species. Intraspecific competition is closely tied to plant density, as higher population levels intensify competition for light, water, and nutrient availability. The field experiment was conducted at the Institute of Plant Protection – National Research Institute, utilizing a rigorous three-factor split-split-plot design with four replications in a randomized complete block design. The first factor included two maize cultivars, 'Wilga' and 'Wigo', which differed in their vegetation period according to the FAO maturity scale. The second factor involved plant arrangement patterns, specifically square and rectangular. The third factor was plant density, set at 5, 7, and 10.5 plants·m^{-2} corresponding to 50,000, 70,000, and 105,000 plants per hectare, respectively. This study showed that plant spatial arrangement and population density strongly influenced maize morphology, canopy structure, and yield by affecting intraspecific competition and resource use. The square planting pattern outperformed the conventional rectangular pattern, promoting more uniform canopies, better light distribution, and improved resource efficiency, resulting in more consistent yields at moderate densities. Certain hybrids performed better under high density conditions.

Keywords: canopy structure, grain yield, intraspecific competition, leaf area index (LAI), plant density, plant morphology, planting pattern, spatial arrangement, yield components

Introduction

Maize (*Zea mays* L.) is one of the most important cultivated crops in the world, alongside wheat and rice. It serves as a fundamental raw material for food, feed, and industrial purposes. On a global scale, it represents a crucial component of food and economic systems. It is used as animal feed, a raw material for producing starch, syrups, bioethanol, and other industrial products, and as a food ingredient for humans (Shiferaw *et al.* 2013; Ranum *et al.* 2014; Erenstein *et al.* 2022). Current evidence indicates that the strategic role of maize in global food systems is increasingly linked to the need for improving resource-use efficiency under intensified production systems, particularly through optimization of canopy structure and photosynthetic performance at the population level (Azrai *et al.* 2025). Moreover, long-term studies emphasize that overall plant health and crop management practices are fundamental for sustaining maize productivity and yield stability under field conditions (Michalski *et al.* 2000). The economic importance of maize also stems from its flexibility; it can be cultivated under diverse climatic and soil conditions and serves as an essential element of agroecological systems (e.g., intercropping and soil structure-improving plants). In recent decades, a systematic increase in the maize cultivation area has been observed, especially in developing countries. This growth is linked to rising demands for animal feed and biofuels, as well as the development of varieties resistant to environmental stresses and more efficient in using soil resources (Abate *et al.* 2015; Badu-Apraku *et al.* 2023). In parallel with these trends, research has reported that agronomic and environmental factors jointly influence maize growth and productivity, reinforcing the importance of integrated crop management in modern maize production systems (Kucharczyk *et al.* 2011; Bereś 2012). One of the crucial factors influencing maize grain and biomass yield is plant density, i.e., the number of plants per unit area. An appropriate plant stand determines the degree of utilization of light, water, and nutrients and defines the balance between vegetative and generative growth (Çakir 2004). Optimal sowing density depends on habitat conditions, cultivation system, and applied technology (irrigation, fertilization, cultivar). In temperate and Mediterranean climates, the typical recommended density for grain varieties ranges from 75,000 to 90,000 plants·ha^{-1}, whereas for forage varieties it may exceed 100,000 plants·ha^{-1} (Maresma *et al.* 2019). Experimental findings from recent years demonstrate that fine-tuning planting density, particularly when combined with optimized nitrogen management, leads to measurable improvements in canopy structure, intercepted photosynthetically active radiation (IPAR), and photosynthetic capacity, resulting in enhanced biomass accumulation and grain yield (Lai *et al.* 2025). In recent years, both breeding progress

and advancements in maize cultivation technology have led to a systematic increase in plant density within stands. The objective of this practice is to maximize the use of available resources, primarily sunlight, by increasing the total leaf area capable of intercepting photosynthetically active radiation (PAR) (Toler *et al.* 1999; Song *et al.* 2016; Wang *et al.* 2021). Evidence from controlled and field-based experiments shows that planting strategies integrating plant density with spatial arrangement regulate canopy light distribution, delay leaf senescence, and enhance net photosynthetic rates, thereby improving productivity in dense maize stands (Zhao *et al.* 2025). However, the increase in plant number per unit area does not translate linearly into yield growth, as plants in dense stands begin to compete for light, water, and nutrients, leading to a reduction in the yield of individual plants. Consequently, the number and length of ears, thousand-kernel weight, and overall individual productivity decrease (Testa *et al.* 2016). This intraspecific competition is an important factor in determining maize productivity, canopy structure, and the efficiency of resource utilization. Under field conditions, the intensity of this competition increases with higher plant density per unit area, affecting canopy architecture, light availability, photosynthetic processes, and final grain yield. This phenomenon results from limited space and resource availability mainly, light, water, and minerals, and leads to variable plant development within a population, manifested by changes in plant height, internode length, leaf assimilation area, and stem branching degree (Li *et al.* 2018).

Such density-induced morphological and physiological responses are increasingly regarded as important targets in breeding programs aimed at improving tolerance to dense planting and enhancing light-use efficiency at the canopy level (Azrai *et al.* 2025). Plant density is thus a significant factor shaping canopy structure and the interception of photosynthetically active radiation (PAR). Under high-density conditions, competition for light intensifies, leading to stem elongation and a more vertical orientation of leaf blades, which enables more efficient light utilization in the upper canopy layers. This process, known as the morphological adaptation of the canopy to light stress, results from selective competition among individuals. However, it is accompanied by decreased photosynthetic efficiency in lower plant parts due to limited light availability (Toler *et al.* 1999; Song *et al.* 2016; Wang *et al.* 2021). Canopy-level analyses further emphasize that maintaining plant vigor and physiological activity throughout the growing season is essential for stabilizing yield under intensive cultivation systems (Michalski *et al.* 2000). It has been demonstrated that high plant densities lead to changes in biomass allocation, directing a greater portion of assimilates toward vegetative growth. This limits the development of generative organs, including ears, and

consequently reduces unit yield. Increased light competition during early growth stages may cause irreversible yield losses, only partially compensated for by later canopy reorganization and enhanced assimilation efficiency of dominant plants (Page *et al.* 2010). One of the main factors driving increases in maize yield over recent years has been both genetic progress and improvements in agronomic practices. Modern maize cultivars are characterized by much higher plant density than those grown several years ago. These changes were not accidental. Alongside the increase in the productivity of individual plants, the so-called agronomic optimum, i.e., the sowing density that ensures maximum yield per unit area, has also evolved. The higher yields achieved today result not only from the increased number of plants per hectare but also from the fact that new maize hybrids better tolerate stresses associated with higher competition for light, water, and nutrients (Moll *et al.* 1977; Yan *et al.* 2011; Al-Naggar *et al.* 2017).

Accumulating evidence suggests that yield gains in modern hybrids are closely associated with improved physiological stability and overall plant health under intensified production conditions (Bereś 2012; Zhao *et al.* 2025). Since the mid-20th century, maize breeding has focused on traits enabling plants to maintain stable yields at increasingly high stand densities. These include such elements as, more upright leaves, stronger stems, improved root systems, and greater light-use efficiency. However, not only genetics but also cultivation technology, including plant density and spatial arrangement, has played a crucial role in a long-term increase in productivity. In this context, it becomes crucial to ask whether further increases in stand density continue to provide measurable yield benefits, or whether the limit has already been reached, beyond which additional plants compete too vigorously, reducing overall canopy efficiency (Moll *et al.* 1977; Al-Naggar *et al.* 2017; Sangoi 2001). Understanding the interaction between plant number per unit area and unit yield is critical for further improving maize productivity under global conditions. In light of the growing demand for food and limited natural resources, precisely determining the optimal plant stand and developing varieties with high tolerance to stand density have become some of the most important challenges in modern agronomy and maize breeding (Assefa *et al.* 2018). Overall, findings from agronomic, physiological, and plant protection research underline the necessity of integrating stand density optimization with practices supporting overall plant health to further enhance maize productivity under intensified cropping systems (Michalski *et al.* 2000; Azrai *et al.* 2025). The present study aimed to determine the effects of the spatial arrangement of plants for two maize cultivars, sown in square and rectangular patterns at variable plant densities per unit area, on maize yield and plant morphology. The research hypothesis assumed that the spatial

arrangement of plants, the number of plants per unit area, and the cultivar factor determine maize plant morphology and yield (intraspecific competition).

Materials and Methods

2.1. Location of the Experiment and Description of Experimental Objects

The field experiments were conducted at the Experimental Station in Winna Góra (52°12′17″N, 17°26′48″E) in the Institute of Plant Protection – National Research Institute in Poznań, Poland. The study was carried out over three consecutive growing seasons (2015, 2016, and 2017) and included two maize cultivars: Wilga and Wigo. A detailed description of the cultivars is presented in Table 1.

Table 1. Characteristics of maize cultivars

Trait	Cv. Wilga	Cv. Wigo
FAO – for grain production	180	250
Hybrid type	three-way cross (TC)	three-way cross (TC)
Kernel type	semi-flint	semi-flint / semi-dent
Plant vigor at early growth stage	good, early	good, early
Mean plant height	220 cm	250 cm

The experiment included three experimental (independent) factors (Tab. 2, Fig. 1):

- *Main factor*: Two maize cultivars differing in FAO maturity group – Wilga (FAO 180) and Wigo (FAO 250);
- *Second-level factor*: Spatial arrangements (SA): seeding pattern – square (S) and rectangular arrangements (R);
- *Third-level factor*: Plant density – 5, 7, and 10.5 plants·m^{-2}.

The first experimental factor was two maize cultivars differing in FAO maturity group – Wilga (FAO 180) and Wigo (FAO 250). The second experimental factor was the spatial arrangement of maize. In this study, plants were sown in rectangular and square arrangements. The grid spacing was calculated based on the assumed plant density·m^{-2} and the row spacing (a) for a given spatial arrangement. Two spatial arrangements were examined: rectangular and square. When calculating the grid dimensions, the formulas for the area of a rectangle and a square were used: $P = a \cdot b$; $P = a^2$. For the rectangular arrangement, the row spacing (a) between maize

rows was set at three variants: 100, 85, and 70 cm. The third experimental factor was sowing density. Maize was sown at target plant populations of 5, 7, and 10.5 plants·m^{-2}. A density of 5 plants·m^{-2} corresponded to 50,000 plants·ha^{-1}, 7 plants·m^{-2} corresponded to 70,000 plants·ha^{-1}, and 10.5 plants·m^{-2} corresponded to 105,000 plants·ha^{-1} (Fig. 1). The calculations for rectangular and square sowing patterns at the intended plant densities were carried out as follows and are presented in Table 2 and 3. All experimental objects are presented in Table 4.

Rectangular Sowing Pattern

The rectangular sowing pattern (spatial arrangement) was established assuming a given inter-row spacing (a) and calculating the in-row spacing (b) based on the plant density (n, plants·m^{-2}):

$$A = a \times b$$
$$b = \frac{A}{a}$$

where A is the area per plant.

Table 2. Relationship between plant density, inter-row spacing, in-row spacing, and area per plant in a rectangular sowing pattern

Plant density (plants·m^{-2})	Inter-row spacing a (cm)	Area per plant (m² / cm²)	In-row spacing b (cm)
5.0	100	0.20 / 2000	20.0
7.0	85	0.1428 / 1428	16.8
10.5	70	0.0952 / 952	13.6

Square Sowing Pattern

In the square sowing pattern (spatial arrangement), the distance between plants in both directions was equal ($a = b$).

The side of the square corresponding to one plant was calculated as:

$$A = a^2$$
$$a = \sqrt{A}$$

where A was the area per plant.

Table 3. Relationship between plant density, inter-row spacing, in-row spacing, and area per plant in a square sowing pattern

Plant density (plants·m⁻²)	Inter-row spacing a (cm)	Area per plant (m² / cm²)	In-row spacing b (cm)
5.0	100	0.20 / 2000	44.7
7.0	85	0.1428 / 1428	37.8
10.5	70	0.0952 / 952	30.9

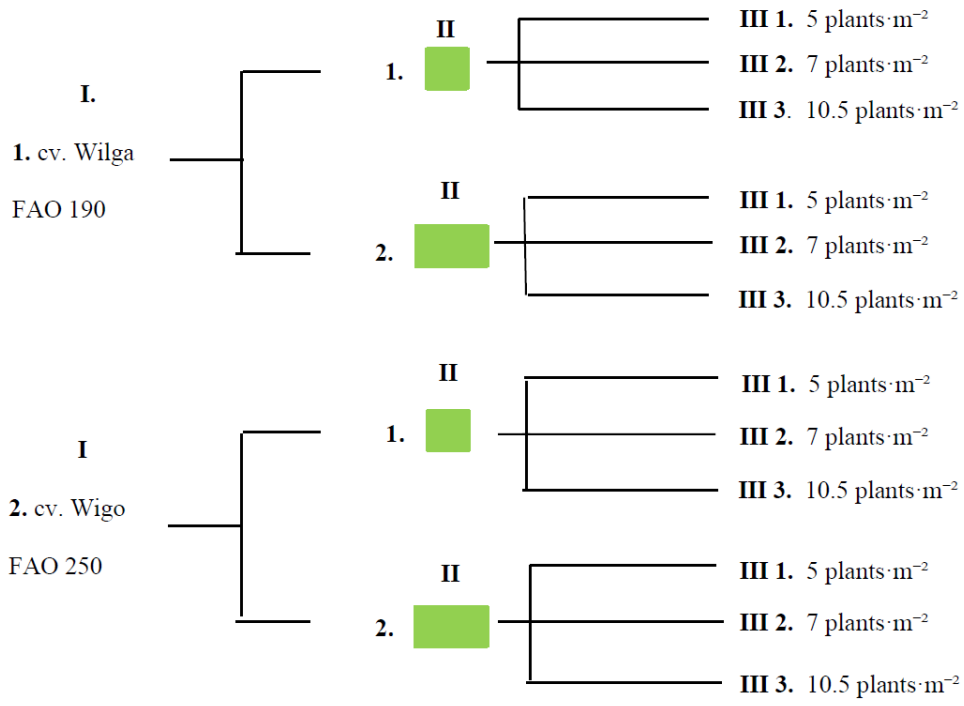

Fig. 1. Experimental design

Table 4. Experimental design and field layout

Symbol	Cultivar	Arrangement	Dimensions (cm)	Sowing Density (plants·m⁻²)
SA-1	Wilga	Rectangular (R)	100 × 20	5
SA-2	Wilga	Square (S)	37.8 × 37.8	7
SA-3	Wilga	Rectangular	70 × 13.6	10.5
SA-4	Wilga	Square	44.7 × 44.7	5
SA-5	Wilga	Rectangular	85 × 16.8	7
SA-6	Wilga	Square	30.9 × 30.9	10.5
SA-7	Wigo	Rectangular	100 × 20	5

SA-8	Wigo	Square	37.8 × 37.8	7
SA-9	Wigo	Rectangular	70 × 13.6	10.5
SA-10	Wigo	Square	44.7 × 44.7	5
SA-11	Wigo	Rectangular	85 × 16.8	7
SA-12	Wigo	Square	30.9 × 30.9	10.5

SA–spatial arrangement

2.2. Agrotechnical Conditions

Maize was cultivated in a plow tillage system, using standard agronomic practices. The forecrop for maize in all years of the study was a winter cereal. In the first year, it was winter rye; in the second and third years, winter wheat. Sowing was carried out during the first 10 days of May. It was performed manually using planting templates (molds) with varying row spacing and seed spacing within the row, according to the assumed sowing densities. The sowing depth was 5 cm. At the two-leaf stage of maize (BBCH 12), the herbicide Mocarz 75 WG was applied at 0.2 kg·ha^{-1} to control dicotyledonous weeds. This herbicide contains two active substances: tritosulfuron and dicamba. Tritosulfuron belongs to the group of triazinylsulfonylurea derivatives, while dicamba is a derivative of benzoic acid. Monocotyledonous weeds were removed mechanically at the 6-leaf stage of maize (BBCH 16). The experiments were established in four replications in a split-split-plot design. The size of each plot was 18 m² (6 × 3 m). The experiment was set up on podzolic soil developed from loamy sand with a similar reaction. Differences in soil reaction were related to the experimental location. In 2015 and 2017, the experiments were conducted on slightly acidic soil, whereas in 2016 they were conducted on acidic soil. The organic matter content, depending on location, ranged from 1.24 to 1.41% d.m. The available macronutrient content was as follows: N – 5.7; P – 13.6; K – 15.8 (mg·100 g^{-1} soil).

2.3. Methodology of analyses and measurements

In the study, the following analysis and measurements were carried out: plant height at the 1st observation (H1), plant height at the 2nd observation (H2), leaf area index (LAI), ear length (EL), kernel-bearing ear length (KBL), ear diameter (ED), thousand kernel weight (TKW), starch content (SC), protein content (PC), fat content (FC), yield (Y).

Maize height – the height of 10 maize plants was measured twice during each growing season. The first measurement was taken at the 4-node stage (BBCH 34). The second measurement was conducted at the end of the flowering stage (BBCH 69). A measuring rod with an accuracy of

1 mm was used. The rod, mounted on a wooden strip, was 3 m long. Results were expressed as the mean height of 10 plants in cm.

Leaf Area Index (LAI) – determined at full flowering of maize (BBCH 65). The LAI was measured using an AccuPAR LP 80 device (Decagon Devices). The index was calculated as the ratio of leaf surface area to ground surface area, allowing the degree of light utilization by plants to be determined. The LAI was also defined as the total projected one-sided area of photosynthetically active tissue (leaves) per unit ground area and was expressed in $m^2 \cdot m^{-2}$.

Assessment of maize yield and grain quality parameters: maize was manually harvested at physiological maturity (BBCH 97). From each plot, 15 consecutive ears were collected from randomly selected sites. Before yield determination, each ear was analyzed for ear weight, ear length, ear diameter, and grain fill.

Ear length – measured with a ruler accurate to 1 mm. Results were presented as the mean length of 15 heads in cm.

Grain fill of ears – determined as the ratio of total cob length to the length of the grain-filled portion, measured with a ruler accurate to 1 mm. Results were presented as the mean grain fill of 15 cobs in cm.

Ear diameter – measured with an electronic caliper accurate to 0.1 cm at the midpoint of the cob. The exact location of measurement was determined with a ruler accurate to 1 mm. Results were expressed as the mean diameter of 15 cobs in cm.

Grain yield – based on the grain weight obtained after threshing the ears. Threshing was performed with a Kruszek-type seed cleaner equipped with a maize threshing attachment. Grain was weighed using a WPT-60 platform scale accurate to 0.02 kg. During weighing, grain moisture was determined with a DRAMIŃSKI GMM moisture meter equipped with an alphanumeric LCD showing species name, moisture content (%), and grain temperature. Yield was expressed in tons per hectare, standardized to 30% grain moisture.

Thousand grain weight (TKW) – determined from a 1.0 L grain sample. From each sample, three subsamples of 200 kernels were counted. Kernel mass was determined using a Sartorius BP 2100S balance accurate to 0.01 g. The result was multiplied by 5 and expressed as the mean thousand-kernel weight in grams.

Quality parameters, including protein, starch, and oil contents, were analyzed using an Infratec 1241 analyzer (FOSS). This device is a near-infrared transmission spectrometer. From a 0.5 kg sample of whole kernels, several parameters were determined simultaneously. The method is based on the absorptive properties of electromagnetic radiation in the near-infrared range, primarily by proteins, oils, and starches. Results were expressed as percentages.

2.4. Meteorological conditions

Meteorological conditions during the growing seasons in which the study was conducted were recorded using measuring instruments. Air temperatures were monitored with the "Aster Met" – Automatic Distributed Telemetry System (ASTER), where the installed logger SM-076 served as the measuring station. Precipitation was recorded with measuring devices of the Institute of Meteorology and Water Management (IMGW) and entered into official Rainfall Observation Logs for the years 2015, 2016, and 2017 (Rainfall Station: Winna Góra, catchment area 185 – Warta River from Prosna to Wełna, elevation 90 m a.s.l.). All measuring devices were located at the Experimental Field Station in Winna Góra, approximately 1.5 km from the experimental field. Table 5 presents mean monthly air temperatures, while Table 6 shows precipitation data recorded during the field experiments, compared with long-term averages. Mean air temperatures during maize growing seasons were similar to long-term averages, with deviations not exceeding 0.4°C. Considerable differences in precipitation were observed across the study years. The lowest rainfall was recorded in the 2015 growing season (338.0 mm), which was 66.0 mm below the long-term average. The highest rainfall (554.0 mm) occurred in 2017, exceeding the long-term average by 150.0 mm.

Table 5. Mean month's air temperatures [°C] in the growing seasons 2015–2017 compared with long-term data from 2005-2014)

	Month								Mean (°C)
Years	**IV**	**V**	**VI**	**VII**	**VIII**	**IX**	**X**	**XI**	
2015	8.7	13.7	16.5	20.0	22.8	15.5	8.1	6.5	14.0
2016	9.3	15.9	19.1	19.5	18.3	16.9	8.3	2.5	13.7
2017	8.0	14.2	18.1	18.6	19.7	13.9	11.1	5.7	13.7
Long term data 2005-2014	9.7	14.1	17.6	20.4	18.6	14.8	9.2	4.7	13.6

Table 6. Monthly sum of precipitation [mm] in the growing season 2015–2017 compared with long-term data from 2005–2014

	Month								Sum (mm)
Years	**IV**	**V**	**VI**	**VII**	**VIII**	**IX**	**X**	**XI**	
2015	20.1	31.9	54.8	99.5	18.5	18.0	30.4	64.3	338.0
2016	25.7	48.2	77.3	116.8	16.6	15.2	106.2	36.4	443.0
2017	35.7	55.1	87.0	107.3	86.3	65.1	77.9	39.4	554.0
Long term data 2005-2014	26.2	64.5	53.8	71.6	75.6	50.4	25.9	35.6	404.0

2.5. Statistical analysis

The normality of the empirical distribution of the observed quantitative traits was tested using the Shapiro–Wilk test (Shapiro and Wilk 1965), and the results were visualized with histograms. ANOVA was conducted to assess the effects of year, cultivar, sowing method, and sowing density, as well as their two-, three-, and four-way interactions on trait variability. For each factor combination, mean values and least significant differences (LSD) were calculated to identify homogeneous groups. Trait distributions, depending on year, sowing method, and cultivar, were illustrated using density plots. Relationships among traits were evaluated with Pearson's correlation coefficients (calculated separately for each year and for all years combined), significance tested at 0.05, 0.01, and 0.001, and visualized in heat maps. Additionally, a multivariate analysis of variance (MANOVA) was applied to verify the joint effects of the experimental factors and their interactions on all traits considered together. Mahalanobis distances and canonical variate analysis were used to illustrate the similarities and differences in sowing methods, sowing densities, and cultivars across years. ANOVA test for tested traits is presented in Table 7.

Results

Plant height (H1)

The mean values across the study years revealed statistically significant differences in trait H1 (Tab. 8). Square planting arrangements generally tended to produce taller plants than rectangular systems. In cv. **Wilga** in 2015, the shortest plants were observed in SA–1, whereas the tallest plants were recorded in SA–2, representing a difference of 10.5%. In 2016, the shortest plants were found in SA–6, corresponding to the highest sowing density, whereas the tallest plants occurred in SA–4. In cv. **Wigo**, square arrangements also generally resulted in taller plants. The tallest plants overall were recorded in 2017. In cv. **Wilga**, the lowest plant height was observed in SA–1 and the highest in SA–2, representing a difference of 14.5%, whereas in cv. **Wigo** the most favorable arrangement was SA–8. Analysis of the 3-year averages showed no statistically significant differences between cultivars. Trait distribution differed between cultivars: values for cv. **Wigo** were concentrated around ~205 cm, whereas values for cv. **Wilga** were concentrated around ~190 cm (Fig. 2). Rectangular systems exhibited greater variability, with the highest frequency of observations around ~150 cm, whereas square systems were concentrated around ~190 cm. Regarding sowing density, the greatest variability occurred at 7 plants·m^{-2}, whereas the main concentrations were observed around ~180 cm for 5 plants·m^{-2} and around ~192 cm for both 7 and 10.5 plants·m^{-2}. The greatest year-to-year variability occurred in 2016, while the highest frequency of observations was recorded around ~162 cm in 2015, ~130 cm in 2016, and ~190 cm in 2017. Trait H1 showed statistically significant positive correlations with EL and KBL (Fig. 3).

Plant height (H2)

The mean values of trait H2, presented in Table 9, showed statistically significant differences both within individual years and for the combined 3-year period. In 2017, H2 measurements were not conducted due to unfavorable field conditions during the scheduled assessment period. Taller plants were generally observed in square sowing arrangements. For the 3-year averages in cv. **Wilga**, the tallest plants were recorded in SA–2, whereas the shortest plants were observed in SA–1, with a difference of 11.9% between treatments. In cv. **Wigo**, the tallest plants were observed in SA–8 and the shortest in SA–11 (7 plants·m^{-2}), resulting in a difference of 8.6%. The distribution of H2 values varied depending on the experimental factors. Cv. **Wigo** exhibited greater variability, with the highest frequency of observations around ~205 cm.

Differences in variability were also observed between spatial arrangements. Regarding sowing density, similar ranges of H2 values were observed for all three densities, although the distribution differed: approximately ~155 cm for 5 plants·m^{-2}, ~150 cm and ~205 cm for 7 plants·m^{-2}, and ~205 cm for 10.5 plants·m^{-2} (Fig. 4). Significant differences between years were also observed. In 2015, H2 values ranged from 165 to 230 cm, with the highest frequency around ~205 cm, whereas in 2016 the range narrowed to 150–180 cm, with observations concentrated around ~155 cm.

Leaf Area Index (LAI)

The mean values of the studied treatments across individual years and for the 3-year period (Tab. 10) showed statistically significant differences. In cv. **Wilga**, the highest LAI in 2015 was observed in SA–4, whereas the lowest value was recorded in SA–6, representing a difference of 88.0%. In 2016, the highest LAI occurred in SA–2 and was approximately 7.8-fold higher than the value observed in SA–5. During the wet season of 2017, SA–6 exhibited the highest LAI values, whereas SA–1 showed the lowest values, with a difference of 127.5%. In cv. **Wigo**, the highest LAI in 2015 was recorded in SA–11. In the following two years, the highest values were observed in SA–12 (10.5 plants·m^{-2}), whereas the lowest values occurred in SA–7. The values were approximately 6-fold and 1.6-fold higher, respectively. The distribution of LAI values varied depending on the experimental factors (Fig. 5). Cv. **Wigo** exhibited greater variability, whereas the highest frequency of observations for both cultivars occurred around ~0.8 m^2·m^{-2}. Square systems exhibited broader variability than rectangular arrangements. The widest range of values occurred at the sowing density of 10.5 plants·m^{-2}. Among the study years, the broadest LAI range was recorded in 2015, with the highest frequency around ~2.1 m^2·m^{-2}. The narrowest range occurred in 2017, with observations concentrated around ~0.8 m^2·m^{-2}. Statistically significant positive correlations were found between LAI and ED and ZB (Fig. 3).

Ear length (EL)

The mean values obtained across years, as well as for the 3-year average (Tab. 11), showed statistically significant differences between treatments. In cv. **Wilga**, the square arrangement SA–4 consistently produced the highest EL values throughout all study years. Increases in ear length compared with the lowest observed values amounted to 15.9%, 43.3%, and 13.2% in successive years. The 3-year average also identified SA–4 as the best-performing treatment,

with values 17.5% higher than those recorded in SA–5. Compared with SA–1, representing the same sowing density (5 plants·m^{-2}), SA–4 showed a 4.6% increase, although this difference was not statistically significant. In cv. **Wigo**, the highest EL values were observed in the square arrangement 44.7 × 44.7 cm (SA–10). Increases compared with the lowest values reached 13.8%, 41.5%, and 11.8% in successive years (SA–12, SA–9, and SA–12), respectively. The 3-year average again confirmed SA–10 as the best-performing treatment, with values 21.0% higher than those observed in SA–9. Compared with SA–7, representing the same sowing density, SA–10 showed a 2.1% increase, which was not statistically significant. The distribution of EL values differed considerably among experimental factors. Cv. **Wigo** exhibited greater variability, with the highest frequency of observations around 19 cm. Rectangular systems displayed the widest ranges of values. Regarding sowing density, the greatest variability occurred at 5 plants·m^{-2}. Across the study years, the greatest variability was observed in 2016, with the highest frequency of observations around ~17.5 cm in 2015, ~18 cm in 2016, and ~17.5 cm in 2017 (Fig. 6).

Kernel-bearing ear length (KBL)

The mean values of trait KBL (Tab. 12) showed statistically significant differences across years and for the 3-year average. In cv. **Wilga**, the highest KBL values in 2015 and 2016 were recorded in SA–4. In 2015, SA–4 exceeded the lowest value, observed in SA–3, by 25.4%, whereas in 2016 it exceeded the lowest value, recorded in SA–6, by 25.3%. In 2017, the highest KBL was observed in SA–2, while the lowest value occurred in SA–6, with a difference of 29.5%. The 3-year average indicated the highest KBL in SA–4; however, SA–1 and SA–2 achieved similar values. In cv. **Wigo**, the highest KBL values were consistently observed in SA–10, exceeding the lowest values by 21.8%, 36.9%, and 31.9% across successive years. The 3-year average also identified SA–10 as the most favorable treatment, with values 30.1% higher than those recorded in SA–9 and 3.5% higher than those observed in SA–7, representing the same sowing density, although the latter difference was not statistically significant. Trait KBL exhibited the greatest variability in cv. **Wigo**, with the highest frequency of observations around 17.5 cm. Rectangular systems displayed broader ranges of values, and the greatest variability occurred at 7 plants·m^{-2}. The highest overall variability was observed in 2016 (Fig. 3 and 7).

Ear diameter (ED)

The mean ED values (Tab. 13) showed statistically significant differences across years. Within cv. **Wilga**, the highest ED values in 2015 were observed in SA–1 and SA–4 (5 plants·m^{-2}), with no statistically significant differences between them. In 2016 and 2017, SA–4 produced the highest ED values, exceeding the lowest treatments by 5.3% and 4.2%, respectively. The 3-year average also favored SA–4, which exceeded SA–3 (the lowest treatment) by 4.8%. Compared with SA–1 (the same density), the increase was 0.7%, although it was not statistically significant. In cv. **Wigo**, the highest ED values in 2015 and 2016 were observed in SA–10, although the differences between treatments were not statistically significant. In 2016, SA–10 exceeded SA–12 (the lowest treatment) by 1.8% and SA–7 (the same density) by 1.2%. In 2017, the highest ED values were recorded in SA–7, again without statistically significant differences. The 3-year averages confirmed the highest ED values in SA–10, although differences between treatments remained non-significant. The greatest variability was observed in cv. **Wigo**, under square arrangements, and at a density of 5 plants·m^{-2}. The highest overall variability occurred in 2015, with the highest frequency of observations around 4.25 cm in 2015 and 2017, and around 4.30 cm in 2016 (Fig. 8).

Thousand Kernel Weight (TKW)

The mean TKW values showed significant differences between experimental treatments in 2016 and 2017, whereas no significant differences were found in cv. **Wilga** and cv. **Wigo** in 2015 (Tab. 14). In cv. **Wilga**, the highest TKW in 2016 was recorded in SA–2, while the lowest value occurred in SA–5, with a difference of 7.8%. In 2017, the highest TKW was observed in SA–1 and the lowest in SA–6, resulting in a difference of 12.0%. The 3-year mean showed no statistically significant differences in cv. **Wilga**. In cv. **Wigo**, the highest TKW values in 2016 and 2017 were recorded in SA–7, exceeding the lowest values by 9.5% and 11.3%, respectively. The 3-year mean also indicated the highest TKW in SA–7, which was 7.6% higher than in SA–9. Higher numerical TKW values were observed in cv. **Wigo** than in cv. **Wilga**. Among spatial arrangements, square systems showed greater variability, with the highest frequency of observations around 320 g (Fig. 9). Regarding sowing density, concentrations were observed around ~320 g at 5 and 10.5 plants·m^{-2} and around ~325 g at 7 plants·m^{-2}. The broadest variation occurred in 2015, with the lowest concentration around ~280 g, whereas in 2016 and 2017 values were concentrated around ~325 g and ~320 g, respectively. A positive and statistically significant correlation between TKW and KBL was observed (Fig. 3).

Starch Content (SC)

The 3-year mean values of SC showed no statistically significant differences, although significant differences were observed in individual years (Tab. 15). In cv. **Wilga**, the highest values in 2016 were observed in SA–3 and SA–5, which exceeded SA–4 by approximately 1.1%. In 2017, the highest SC was recorded in SA–6 and the lowest in SA–4, representing a difference of 1.5%. However, the 3-year averages showed no statistically significant differences between treatments. In cv. **Wigo**, the highest SC in 2015 was observed in SA–12, whereas the lowest value occurred in SA–11, and the difference was statistically significant. In 2016 and 2017, the highest values were observed in SA–9, although the differences were not statistically significant. The 3-year averages again showed no statistically significant differences. SC distribution was broader in cv. **Wigo**, whereas spatial arrangement and sowing density did not substantially affect this trait. The greatest yearly variability was observed in 2015, with the highest frequency of observations around ~57%, whereas in 2016 and 2017 values were concentrated around ~70% (Fig. 10). No statistically significant correlations were found.

Protein Content (PC)

Significant differences were observed between the studied treatments (Tab. 16). In cv. **Wilga**, the highest PC value in 2015 was observed in SA–2, whereas the lowest value occurred in SA–5; both treatments represented the sowing density of 7 plants·m^{-2}, and the difference amounted to 9.7%. In 2016 and 2017, the highest PC values were recorded in SA–4, exceeding SA–3 and SA–6 by 12.4% and 14.4%, respectively. The 3-year averages confirmed SA–4 as the most favorable treatment and SA–6 as the least favorable, with a difference of 10.4%. Compared with SA–1, representing the same sowing density (5 plants·m^{-2}), SA–4 showed a 2.5% increase, although this difference was not statistically significant. In cv. **Wigo**, the highest PC values were observed in SA–7 in both 2015 and 2017. In 2015, SA–7 exceeded SA–12 by 16.8%, whereas in 2017 it exceeded SA–9 by 12.7%. The 3-year averages showed the highest PC values in low-density treatments (5 plants·m^{-2}: SA–7 and SA–10), which were 12.9% higher than those recorded in SA–9 (10.5 plants·m^{-2}). PC variability was greater in cv. **Wilga**, whereas spatial arrangement did not substantially affect this trait (Fig. 11). The lowest variability occurred at 5 plants·m^{-2}. The greatest yearly variability was observed in 2015, whereas the lowest variability occurred in 2017, with the highest frequency of observations around 11.9% in 2015, 10.2% in 2016, and 9.1% in 2017. A positive correlation between PC and EL was observed (Fig. 3).

Fat Content (FC)

Significant differences were observed between the studied treatments (Tab. 17). In cv. **Wilga**, no statistically significant differences were observed in 2015. In 2016 and 2017, the highest FC values were recorded in SA–4. In 2016, SA–4 exceeded the lowest value, observed in SA–3, by 4.5%, whereas in 2017 it exceeded the lowest value, observed in SA–5, by 7.7%. The 3-year averages identified SA–4 as the most favorable treatment. In cv. **Wigo**, among the highest FC values in 2015 were those recorded in SA–7 and SA–10. In 2016, the highest FC was observed in SA–10, whereas in 2017 the highest value occurred in SA–8. The 3-year averages showed the highest FC values in SA–10, which exceeded SA–9 by 4.9%; compared with SA–7, the difference was not statistically significant. FC variability was greater in cv. **Wigo** under square arrangements, whereas the greatest variability was observed at a density of 10.5 plants·m^{-2} (Fig. 12). The greatest yearly variability was observed in 2015, whereas the lowest variability occurred in 2017. Positive correlations were observed between FC and both KBL and ED.

Yield (Y)

The mean values of the studied treatments, both across years and for the 3-year average (Fig. 13), showed statistically significant differences. For the cv. **Wilga**, the highest average yield over three years was obtained in SA–6 and the lowest in SA–1, with a difference of 57.8%. Yield increased notably in square arrangements: at densities of 5, 7, and 10.5 plants·m^{-2}, yields were higher by 7.3%, 7.9%, and 3.8%, respectively. For the cv. **Wigo**, square arrangements were also more favorable. The highest yield was achieved in SA–12 (highest density), which exceeded the rectangular system with the same density (SA–9) by 12.62%, corresponding to an increase of 1.21 t·ha^{-1}. The distribution of yield values varied with experimental factors. **Wigo** showed greater variability, with peak accumulation around 6.8 t·ha^{-1}, while **Wilga** was concentrated around 5.9 t·ha^{-1} (Fig. 14). Rectangular arrangements displayed wider variability. Plant density values were ~6.3 t·ha^{-1} for 5 plants·m^{-2}, and ~7 t·ha^{-1} for both 7 and 10.5 plants·m^{-2}. The most significant variability and accumulation were observed in 2015 (~9.5 t·ha^{-1}), while the peak values in subsequent years were 6.7 t·ha^{-1} in 2016 and 6.5 t·ha^{-1} in 2017. For yield (Y), a statistically significant negative correlation was recorded with KBL and ZB (Fig. 3).

Table 8. Maize height during the 1st observation

Symbol	Cultivar	Arrangement	Number of plants·m^{-2}	Maize height 1st observation (cm)			
				Year			
				2015	2016	2017	2015-2017
SA-1	Wilga	R 100 x 20	5	178.6^{bcde}	141.8^{abcd}	181.6^{f}	167.3^{a}
SA-2	Wilga	S 37.8 x 37.8	7	197.4^{a}	143.5^{abcd}	208.0^{bc}	182.9^{a}
SA-3	Wilga	R 70 x 13.6	10.5	183.4^{abc}	132.8^{abcd}	196.2^{de}	170.8^{a}
SA-4	Wilga	S 44.7 x 44.7	5	182.1^{abcd}	156.9^{a}	192.8^{de}	177.3^{a}
SA-5	Wilga	R 85 x 16.8	7	183.0^{abc}	137.9^{abcd}	187.8^{ef}	169.6^{a}
SA-6	Wilga	S 30.9 x 30.9	10.5	190.1^{ab}	131.7^{bcd}	193.1^{de}	171.7^{a}
SA-7	Wigo	R 100 x 20	5	170.3^{cdef}	123.2^{d}	209.4^{abc}	167.6^{a}
SA-8	Wigo	S 37.8 x 37.8	7	175.1^{bcdef}	153.7^{ab}	217.0^{a}	181.9^{a}
SA-9	Wigo	R 70 x 13.6	10.5	168.8^{cdef}	127.4^{cd}	197.9^{d}	164.7^{a}
SA-10	Wigo	S 44.7 x 44.7	5	164.7^{ef}	148.8^{abc}	200.6^{cd}	171.3^{a}
SA-11	Wigo	R 85 x 16.8	7	162.9^{f}	120.8^{d}	212.9^{ab}	165.5^{a}
SA-12	Wigo	S 30.9 x 30.9	10.5	166.1^{def}	142.3^{abcd}	207.4^{bc}	171.9^{a}
	$LSD_{0.05}$			*16.11*	*24.16*	*8.93*	*24.7*

SA–spatial arrangement; R—rectangular; S—square

Table 9. Maize height during the 2nd observation

Symbol	Cultivar	Arrangement	Number of plants·m^{-2}	Maize height 2nd observation *(*cm)			
				Year			
				2015	2016	2017	2015-2017
SA-1	Wilga	R 100 x 20	5	179.2^{d}	159.1^{d}	-	169.2^{c}
SA-2	Wilga	S 37.8 x 37.8	7	202.4^{ab}	176.4^{abcd}	-	189.4^{abcd}
SA-3	Wilga	R 70 x 13.6	10.5	189.2^{bcd}	165.8^{cd}	-	177.5^{de}
SA-4	Wilga	S 44.7 x 44.7	5	196.2^{abc}	174.5^{abcd}	-	185.4^{bcd}
SA-5	Wilga	R 85 x 16.8	7	195.2^{abc}	170.8^{bcd}	-	183.0^{cd}
SA-6	Wilga	S 30.9 x 30.9	10.5	184.2^{cd}	170.8^{bcd}	-	177.5^{de}
SA-7	Wigo	R 100 x 20	5	206.9^{a}	180.9^{abc}	-	193.9^{abc}
SA-8	Wigo	S 37.8 x 37.8	7	205.6^{a}	195.1^{a}	-	200.3^{a}
SA-9	Wigo	R 70 x 13.6	10.5	205.2^{a}	188.6^{ab}	-	196.9^{ab}
SA-10	Wigo	S 44.7 x 44.7	5	195.8^{abc}	182.0^{abc}	-	188.9^{abcd}
SA-11	Wigo	R 85 x 16.8	7	193.2^{abc}	175.6^{abcd}	-	184.4^{bcd}
SA-12	Wigo	S 30.9 x 30.9	10.5	206.5^{a}	192.0^{ab}	-	199.2^{a}
	$LSD_{0.05}$			*15.81*	*21.5*		*13*

SA–spatial arrangement; R—rectangular; S—square
H2 measurements were not available in 2017 due to unfavorable conditions during the assessment period.

Table 10. Leaf Area Index (LAI) in maize

Symbol	Cultivar	Arrangement	Number of plants·m^{-2}	Leaf Area Index (LAI)			
				Year			
				2015	2016	2017	2015-2017
SA-1	Wilga	R 100 x 20	5	2.197^{cde}	0.482^{def}	0.545^{fg}	1.075^{ab}
SA-2	Wilga	S 37.8 x 37.8	7	2.005^{de}	2.195^{a}	0.873^{cd}	1.691^{ab}
SA-3	Wilga	R 70 x 13.6	10.5	1.522^{e}	1.163^{bcd}	0.927^{bc}	1.204^{ab}
SA-4	Wilga	S 44.7 x 44.7	5	2.737^{bcde}	1.780^{abc}	0.772^{cdef}	1.763^{ab}
SA-5	Wilga	R 85 x 16.8	7	1.645^{e}	0.250^{f}	0.688^{def}	0.861^{b}
SA-6	Wilga	S 30.9 x 30.9	10.5	1.455^{e}	1.103^{cde}	1.240^{a}	1.266^{ab}
SA-7	Wigo	R 100 x 20	5	3.382^{abc}	0.263^{f}	0.427^{g}	1.357^{ab}
SA-8	Wigo	S 37.8 x 37.8	7	3.660^{ab}	0.722^{def}	0.825^{cde}	1.736^{ab}
SA-9	Wigo	R 70 x 13.6	10.5	2.375^{bcde}	1.005^{de}	0.875^{cd}	1.418^{ab}
SA-10	Wigo	S 44.7 x 44.7	5	3.345^{abcd}	0.910^{def}	0.585^{fg}	1.613^{ab}
SA-11	Wigo	R 85 x 16.8	7	4.238^{a}	0.453^{ef}	0.630^{efg}	1.773^{ab}
SA-12	Wigo	S 30.9 x 30.9	10.5	2.633^{bcde}	1.847^{ab}	1.118^{ab}	1.866^{a}
	$LSD_{0.05}$			*1.34*	*0.6939*	*0.2303*	*0.9433*

SA–spatial arrangement; R–rectangular; S–square

Table 11. Ear length of maize

Symbol	Cultivar	Arrangement	Number of plants·m^{-2}	Ear length of maize (cm)			
				Year			
				2015	2016	2017	2015-2017
SA-1	Wilga	R 100 x 20	5	17.38^{abc}	16.37^{de}	17.82^{cde}	17.19^{c}
SA-2	Wilga	S 37.8 x 37.8	7	17.65^{abc}	15.61^{ef}	18.37^{abc}	17.21^{c}
SA-3	Wilga	R 70 x 13.6	10.5	15.80^{d}	14.13^{fg}	16.42^{g}	15.45^{d}
SA-4	Wilga	S 44.7 x 44.7	5	18.32^{a}	17.05^{cde}	18.59^{abc}	17.99^{abc}
SA-5	Wilga	R 85 x 16.8	7	16.72^{cd}	11.90^{h}	17.31^{def}	15.31^{d}
SA-6	Wilga	S 30.9 x 30.9	10.5	15.80^{d}	13.75^{g}	16.71^{fg}	15.42^{d}
SA-7	Wigo	R 100 x 20	5	18.02^{ab}	19.22^{a}	18.77^{ab}	18.67^{ab}
SA-8	Wigo	S 37.8 x 37.8	7	16.92^{bcd}	18.89^{ab}	17.84^{cde}	17.88^{bc}
SA-9	Wigo	R 70 x 13.6	10.5	16.20^{d}	13.84^{g}	17.18^{efg}	15.74^{d}
SA-10	Wigo	S 44.7 x 44.7	5	18.46^{a}	19.58^{a}	19.13^{a}	19.06^{a}
SA-11	Wigo	R 85 x 16.8	7	17.72^{abc}	18.39^{abc}	18.10^{bcd}	18.07^{abc}
SA-12	Wigo	S 30.9 x 30.9	10.5	16.88^{bcd}	17.41^{bcd}	17.11^{efg}	17.13^{c}
	$LSD_{0.05}$			*1.17*	*1.52*	*0.84*	*1.1*

SA–spatial arrangement; R–rectangular; S–square

Table 12. Kernel-bearing ear length of maize

Symbol	Cultivar	Arrangement	Number of plants·m^{-2}	Kernel-bearing ear length (cm)			
				Year			
				2015	2016	2017	2015-2017
SA-1	Wilga	R 100 x 20	5	16.00^{abc}	15.34^{cd}	16.79^{ab}	16.08^{bc}
SA-2	Wilga	S 37.8 x 37.8	7	16.32^{abc}	14.57^{cde}	17.33^{a}	16.07^{bc}
SA-3	Wilga	R 70 x 13.6	10.5	13.80^{d}	12.46^{f}	15.05^{cd}	13.77^{def}
SA-4	Wilga	S 44.7 x 44.7	5	17.30^{a}	15.36^{cd}	16.67^{ab}	16.44^{bc}
SA-5	Wilga	R 85 x 16.8	7	14.99^{cd}	14.18^{de}	15.02^{cd}	14.73^{d}
SA-6	Wilga	S 30.9 x 30.9	10.5	13.85^{d}	12.26^{f}	13.38^{e}	13.16^{f}
SA-7	Wigo	R 100 x 20	5	16.69^{abc}	17.13^{ab}	17.31^{ab}	17.04^{ab}
SA-8	Wigo	S 37.8 x 37.8	7	15.22^{bcd}	16.18^{bc}	15.86^{bc}	15.75^{c}
SA-9	Wigo	R 70 x 13.6	10.5	13.79^{d}	13.38^{ef}	13.50^{e}	13.56^{ef}
SA-10	Wigo	S 44.7 x 44.7	5	16.80^{ab}	18.32^{a}	17.80^{a}	17.64^{a}
SA-11	Wigo	R 85 x 16.8	7	15.87^{abc}	16.08^{bc}	16.37^{abc}	16.11^{bc}
SA-12	Wigo	S 30.9 x 30.9	10.5	14.10^{d}	15.14^{cd}	14.37^{de}	14.53^{de}
	$LSD_{0.05}$			*1.76*	*1.68*	*1.34*	*0.99*

SA–spatial arrangement; R—rectangular; S—square

Table 13. Ear diameter of maize

Symbol	Cultivar	Arrangement	Number of plants·m^{-2}	Ear diameter of maize (cm)			
				Year			
				2015	2016	2017	2015-2017
SA-1	Wilga	R 100 x 20	5	4.287^{b}	4.298^{bcd}	4.302^{bc}	4.296^{b}
SA-2	Wilga	S 37.8 x 37.8	7	4.242^{b}	4.288^{cd}	4.242^{cd}	4.257^{bc}
SA-3	Wilga	R 70 x 13.6	10.5	4.090^{b}	4.153^{e}	4.147^{d}	4.130^{d}
SA-4	Wilga	S 44.7 x 44.7	5	4.285^{b}	4.375^{abc}	4.320^{bc}	4.327^{b}
SA-5	Wilga	R 85 x 16.8	7	4.200^{b}	4.210^{de}	4.188^{cd}	4.199^{cd}
SA-6	Wilga	S 30.9 x 30.9	10.5	4.102^{b}	4.252^{d}	4.183^{cd}	4.179^{cd}
SA-7	Wigo	R 100 x 20	5	4.593^{a}	4.390^{a}	4.533^{a}	4.506^{a}
SA-8	Wigo	S 37.8 x 37.8	7	4.545^{a}	4.382^{ab}	4.522^{a}	4.483^{a}
SA-9	Wigo	R 70 x 13.6	10.5	4.497^{a}	4.367^{abc}	4.462^{a}	4.442^{a}
SA-10	Wigo	S 44.7 x 44.7	5	4.632^{a}	4.442^{a}	4.512^{a}	4.528^{a}
SA-11	Wigo	R 85 x 16.8	7	4.540^{a}	4.370^{abc}	4.417^{ab}	4.442^{a}
SA-12	Wigo	S 30.9 x 30.9	10.5	4.585^{a}	4.365^{abc}	4.515^{a}	4.488^{a}
	$LSD_{0.05}$			*0.2*	*0.09*	*0.14*	*0.09*

SA–spatial arrangement; R—rectangular; S—square

Table 14. Maize thousand grain weight

Symbol	Cultivar	Arrangement	Number of plants·m^{-2}	Thousand grain weight (g)			
				Year			
				2015	2016	2017	2015-2017
SA-1	Wilga	R 100 x 20	5	286.6^{b}	320.2^{i}	351.7^{bcd}	319.5^{c}
SA-2	Wilga	S 37.8 x 37.8	7	294.6^{b}	329.3^{g}	317.1^{e}	313.7^{c}
SA-3	Wilga	R 70 x 13.6	10.5	278.6^{b}	325.5^{h}	327.9^{de}	310.7^{c}
SA-4	Wilga	S 44.7 x 44.7	5	286.7^{b}	325.2^{h}	332.5^{cde}	314.8^{c}
SA-5	Wilga	R 85 x 16.8	7	283.2^{b}	305.4^{k}	320.3^{de}	303.0^{c}
SA-6	Wilga	S 30.9 x 30.9	10.5	275.2^{b}	316.5^{j}	314.1^{e}	301.9^{c}
SA-7	Wigo	R 100 x 20	5	359.5^{a}	398.9^{a}	403.7^{a}	387.4^{a}
SA-8	Wigo	S 37.8 x 37.8	7	359.6^{a}	373.6^{d}	382.5^{ab}	371.9^{ab}
SA-9	Wigo	R 70 x 13.6	10.5	348.3^{a}	369.0^{e}	362.6^{bc}	360.0^{b}
SA-10	Wigo	S 44.7 x 44.7	5	361.4^{a}	383.5^{b}	378.8^{ab}	374.5^{ab}
SA-11	Wigo	R 85 x 16.8	7	357.3^{a}	378.1^{c}	363.7^{bc}	366.4^{b}
SA-12	Wigo	S 30.9 x 30.9	10.5	347.4^{a}	364.4^{f}	381.4^{ab}	364.4^{b}
	$LSD_{0.05}$			*22.85*	*3.11*	*33.69*	*18.94*

SA–spatial arrangement; R–rectangular; S–square

Table 15. Starch content in maize grain

Symbol	Cultivar	Arrangement	Number of plants·m^{-2}	Starch content in grain (%)			
				Year			
				2015	2016	2017	2015-2017
SA-1	Wilga	R 100 x 20	5	56.58^{a}	69.97^{abc}	69.9^{bcd}	65.48^{a}
SA-2	Wilga	S 37.8 x 37.8	7	56.70^{a}	69.95^{abc}	70.05^{bc}	65.57^{a}
SA-3	Wilga	R 70 x 13.6	10.5	57.12^{a}	70.42^{a}	69.95^{bcd}	65.83^{a}
SA-4	Wilga	S 44.7 x 44.7	5	56.62^{a}	69.67^{bc}	69.68^{cde}	65.33^{a}
SA-5	Wilga	R 85 x 16.8	7	56.85^{a}	70.42^{a}	70.18^{b}	65.82^{a}
SA-6	Wilga	S 30.9 x 30.9	10.5	57.80^{a}	70.17^{ab}	70.72^{a}	66.23^{a}
SA-7	Wigo	R 100 x 20	5	53.18^{c}	69.42^{cd}	69.33^{e}	63.98^{a}
SA-8	Wigo	S 37.8 x 37.8	7	53.85^{bc}	69.55^{cd}	69.38^{e}	64.26^{a}
SA-9	Wigo	R 70 x 13.6	10.5	53.72^{bc}	69.90^{abc}	70.05^{bc}	64.56^{a}
SA-10	Wigo	S 44.7 x 44.7	5	54.00^{bc}	68.97^{d}	69.60^{de}	64.19^{a}
SA-11	Wigo	R 85 x 16.8	7	53.15^{c}	69.53^{cd}	69.55^{de}	64.08^{a}
SA-12	Wigo	S 30.9 x 30.9	10.5	54.60^{b}	69.42^{cd}	69.73^{cde}	64.58^{a}
	$LSD_{0.05}$			*1.27*	*0.61*	*0.44*	*5.79*

SA–spatial arrangement; R–rectangular; S–square

Table 16. Protein content in maize grain

Symbol	Cultivar	Arrangement	Number of plants·m^{-2}	Protein content in grain (%)			
				Year			
				2015	2016	2017	2015-2017
SA-1	Wilga	R 100 x 20	5	11.95^{ab}	10.47^{abc}	9.78^{a}	10.73^{abc}
SA-2	Wilga	S 37.8 x 37.8	7	12.12^{a}	11.03^{ab}	9.32^{ab}	10.82^{ab}
SA-3	Wilga	R 70 x 13.6	10.5	11.80^{abc}	9.85^{cd}	9.12^{bc}	10.26^{abcde}
SA-4	Wilga	S 44.7 x 44.7	5	12.03^{a}	11.07^{a}	9.90^{a}	11.00^{a}
SA-5	Wilga	R 85 x 16.8	7	11.05^{bcd}	10.02^{c}	9.35^{ab}	10.14^{bcde}
SA-6	Wilga	S 30.9 x 30.9	10.5	11.27^{abcd}	9.95^{cd}	8.65^{c}	9.96^{cdef}
SA-7	Wigo	R 100 x 20	5	11.45^{abc}	10.32^{abc}	9.75^{a}	10.5^{abcd}
SA-8	Wigo	S 37.8 x 37.8	7	10.45^{def}	9.82^{cd}	9.12^{bc}	9.80^{def}
SA-9	Wigo	R 70 x 13.6	10.5	10.07^{ef}	9.18^{d}	8.65^{c}	9.30^{f}
SA-10	Wigo	S 44.7 x 44.7	5	11.30^{abcd}	10.9^{ab}	9.38^{ab}	10.50^{abcd}
SA-11	Wigo	R 85 x 16.8	7	10.88^{cde}	10.20^{bc}	9.07^{bc}	10.05^{bcdef}
SA-12	Wigo	S 30.9 x 30.9	10.5	9.80^{f}	9.88^{cd}	8.88^{bc}	9.52^{ef}
	$LSD_{0.05}$			*0.92*	*0.83*	*0.58*	*0.81*

SA–spatial arrangement; R—rectangular; S—square

Table 17. Fat content in maize grain

Symbol	Cultivar	Arrangement	Number of plants·m^{-2}	Fat content in grain (%)			
				Year			
				2015	2016	2017	2015-2017
SA-1	Wilga	R 100 x 20	5	4.60^{d}	3.92^{cd}	3.55^{e}	4.02^{ab}
SA-2	Wilga	S 37.8 x 37.8	7	4.60^{d}	3.92^{cd}	3.57^{e}	4.03^{ab}
SA-3	Wilga	R 70 x 13.6	10.5	4.57^{d}	3.80^{d}	3.52^{e}	3.98^{b}
SA-4	Wilga	S 44.7 x 44.7	5	4.57^{d}	3.97^{bcd}	3.77^{cd}	4.10^{ab}
SA-5	Wilga	R 85 x 16.8	7	4.52^{d}	3.82^{d}	3.50^{e}	3.96^{b}
SA-6	Wilga	S 30.9 x 30.9	10.5	4.47^{d}	3.82^{d}	3.57^{e}	3.95^{b}
SA-7	Wigo	R 100 x 20	5	5.07^{a}	4.00^{abc}	3.97^{ab}	4.36^{a}
SA-8	Wigo	S 37.8 x 37.8	7	4.95^{abc}	4.10^{a}	4.00^{a}	4.36^{a}
SA-9	Wigo	R 70 x 13.6	10.5	4.87^{bc}	3.97^{bcd}	3.70^{de}	4.18^{ab}
SA-10	Wigo	S 44.7 x 44.7	5	5.05^{ab}	4.20^{a}	3.95^{abc}	4.40^{a}
SA-11	Wigo	R 85 x 16.8	7	4.92^{abc}	4.12^{ab}	3.92^{abc}	4.32^{ab}
SA-12	Wigo	S 30.9 x 30.9	10.5	4.85^{c}	4.15^{a}	3.80^{bcd}	4.26^{ab}
	$LSD_{0.05}$			*0.19*	*0.16*	*0.19*	*0.38*

SA–spatial arrangement; R—rectangular; S—square

Discussion

The results of this study provided robust evidence that spatial plant arrangement and stand density interact to shape maize canopy structure, photosynthetic efficiency, and yield performance. The comparative evaluation of square and rectangular planting patterns at varying densities demonstrated that spatial arrangement uniformity was a crucial determinant of resource-use efficiency and intraspecific competition dynamics. These findings were consistent with recent analyses showing that canopy structure, light interception, and grain yield in maize are strongly associated with planting density through changes in vertical and horizontal leaf orientation (Li *et al.* 2018). Comparable conclusions were reported in studies demonstrating that optimized crop layouts can improve light transmittance and reduce intraspecific competition in maize-based systems (Timlin *et al*. 2014; Feng *et al*. 2024). In the current experiment, the square planting pattern enhanced light distribution within the canopy and improved photosynthetically active radiation (PAR) interception, particularly in the middle canopy layers (Maddonni and Otegui 1996; Tharp and Kells 2001). This structural advantage can be explained by the more equidistant spatial configuration, which reduces shading gradients and promotes a more balanced leaf area index (LAI) distribution across the stand (Maddonni and Otegui 1996; Timlin *et al.* 2014). The present findings were also consistent with previous observations indicating that uniform canopy architecture enhances net photosynthesis by improving light penetration and reducing self-shading (Stewart *et al.* 2003). Moreover, lower light attenuation within geometrically uniform canopies allows deeper leaves to maintain higher photosynthetic activity (Maddonni *et al.* 2001; Timlin *et al.* 2014). Similar effects of row spacing on canopy light capture and yield efficiency were also reported under different environmental conditions (Roth 1997; Tharp and Kells 2001; Haarhoff and Swanepoel 2022).

High-density rectangular configurations, by contrast, intensified vertical competition for light, leading to taller plants with elongated internodes, narrower leaves, and a more stratified canopy profile (Lashkari *et al.* 2011; Greveniotis *et al.* 2019). Functional–structural modeling studies confirmed that such architecture reflects plastic adaptation to light stress through resource reallocation toward stem elongation and leaf inclination adjustments that increase apical dominance (He *et al.* 2021). However, this morphological response incurs a physiological cost, as assimilates invested in stem growth reduce reproductive efficiency and ear development (Voldeng and Bloukman 1975; Lashkari *et al.* 2011). Similar trade-offs between canopy structure and radiation-use efficiency were previously described under delayed or dense

planting conditions (Toler *et al.* 1999; Abuzar *et al.* 2011).

The experimental data also confirmed the nonlinear relationship between plant density and grain yield, supporting classical competition models in which individual plant productivity declines once plant density exceeds the agronomic optimum (Dubas 1988; Szmigiel and Oleksy 2004; Abuzar *et al.* 2011; Sulewska *et al.* 2013). Similar relationships were observed in modern maize hybrids differing in density tolerance and morphological plasticity (Zhai *et al.* 2022). The present study corroborates these observations, showing that hybrids characterized by more erect leaves and compact canopy architecture maintained greater yield stability under crowding stress. Interestingly, the effect of spatial arrangement was most pronounced at intermediate densities, where competition remained moderate and environmental resources were still sufficient to support both vegetative and reproductive growth. At the highest density, even the square arrangement could not fully prevent yield reduction, suggesting that physiological constraints such as root competition and source–sink imbalance became dominant (Abuzar *et al.* 2011; Lashkari *et al.* 2011). High-density stands may substantially restrict root expansion and nutrient acquisition, thereby intensifying intraspecific competition (Li *et al.* 2018; Greveniotis *et al.* 2019).

Recent evidence further indicates that tolerance to high plant density depends on an integrated set of canopy architectural and physiological traits (Voldeng and Bloukman 1975; Maddonni and Otegui 1996). Modern maize genotypes optimized for dense planting maintain yield stability through erectophile leaf orientation, reduced canopy self-shading, and sustained photosynthetic activity within middle and lower canopy layers (Azrai *et al.* 2025). These traits improve radiation distribution throughout the canopy and sustain photosynthetic activity in deeper leaf layers, enabling dense stands to increase light interception without proportionally increasing competition (Maddonni and Otegui 1996; Timlin *et al.* 2014). The present results strongly align with this framework, as square planting systems promoted more uniform canopy architecture, balanced LAI distribution, and improved ear development, particularly at intermediate and high plant densities (Voldeng and Bloukman 1975; Lashkari *et al.* 2011; Sulewska *et al.* 2013). This suggests that planting geometry acted synergistically with genotype-dependent architectural traits, amplifying the benefits of density tolerance rather than compensating for its absence (Voldeng and Bloukman 1975). These interactions may also explain why yield component traits were particularly sensitive to spatial arrangement under elevated competitive pressure (Azrai *et al.* 2025).

The reduction in thousand-kernel weight (TKW) and ear length observed under dense rectangular spacing was consistent with assimilate partitioning models suggesting that shading-

induced competition redirects assimilates toward vegetative organs at the expense of kernel development (Tetio-Kagho and Gardner 1988; Lashkari *et al.* 2011; Sulewska *et al.* 2013). Stronger hierarchical dominance within dense canopies also supports the self-thinning concept, whereby dominant plants monopolize available resources at the expense of subdominant individuals (Maddonni and Otegui 2006). Such dominance hierarchies increase spatial heterogeneity within the stand and consequently reduce yield efficiency per unit biomass. Similar responses were previously documented in maize hybrids differing in crowding tolerance and cultivar era (Sangoi *et al.* 2002; Voldeng and Bloukman 1975). Notably, the negative correlation observed between yield and KBL suggests that yield formation under varying density and spatial configurations may involve compensatory relationships among yield components, where larger ear traits do not necessarily translate into higher stand productivity when plant number and kernel set dynamics become dominant (Voldeng and Bloukman 1975; Szulc *et al.* 2017).

Recent physiological evidence indicates that increasing plant density induces multilevel plastic responses, ranging from adjustments in individual leaf photosynthesis to canopy-scale structural reorganization (Pelech *et al.* 2023; Timlin *et al.* 2014). Such responses may improve whole-stand efficiency under moderate crowding but impose severe metabolic costs under excessive density. In the present study, the optimal performance observed at seven plants·m^{-2} in the square arrangement suggests a balance between maximizing light interception and minimizing interplant competition (Abuzar *et al.* 2011; Dubas 1988). Environmental conditions additionally modified the effects of planting geometry. During wetter growing seasons, higher yields and improved kernel set observed in square arrangements were likely associated with more favorable microclimatic conditions, including lower humidity and reduced canopy temperature, which may have decreased disease incidence and kernel abortion (Ghannoum 2009). Similar density × environment interactions affecting radiation-use efficiency (RUE) have also been reported under varying atmospheric conditions and canopy light stratification (Duan *et al.* 2024; Shen *et al.* 2020; Széles *et al.* 2023).

Beyond canopy architecture alone, recent findings emphasize the temporal dimension of photosynthetic efficiency under high-density cultivation. Optimized planting strategies may significantly increase maize yield by delaying leaf senescence and sustaining photosynthetic activity during grain filling (Zhao *et al.* 2025; Ghannoum 2009). Yield gains under dense stands therefore appear to result not only from increased radiation interception but also from prolonged assimilate supply associated with extended functional leaf lifespan. This mechanism provides a physiological explanation for the higher and more stable yields observed in square planting

arrangements in the present study, particularly at seven and 10.5 plants·m^{-2} (Abuzar *et al.* 2011). By improving light distribution and reducing localized shading stress, equidistant spatial arrangements likely contributed to delayed canopy senescence and enhanced radiation-use efficiency, particularly under favorable moisture conditions (Maddonni and Otegui 1996; Timlin *et al.* 2014). Thus, the benefits of optimized planting geometry extend beyond structural effects and may influence whole-season carbon assimilation dynamics.

Genotypic variation between hybrids also played an important role in density adaptation. The longer-season hybrid demonstrated greater tolerance to crowding stress, likely due to prolonged assimilate accumulation and delayed senescence, consistent with previously proposed density-tolerance frameworks (Assefa *et al.* 2018). The development of modern hybrids adapted to high-density cultivation reflects decades of selection aimed at improving leaf angle, stem rigidity, and root strength, which are essential for maintaining productivity under intensified competition (Zhai *et al.* 2022; Sangoi *et al.* 2002). Recent analyses also emphasize the increasing agronomic and economic importance of specialized maize production systems optimized for planting geometry and resource-use efficiency (Martinez-Ortiz *et al.* 2024). Taken together, these findings supported the emerging paradigm that yield optimization under high-density cultivation depends on the interaction between planting geometry, genotype-specific canopy architecture, and sustained photosynthetic activity throughout the growing season (Voldeng and Bloukman 1975; Maddonni and Otegui 1996; Timlin *et al.* 2014). Recent studies have demonstrated that modern maize production increasingly benefits from traits improving canopy light distribution and delaying leaf senescence, thereby sustaining radiation-use efficiency during critical reproductive stages (Azrai *et al.* 2025; Zhao *et al.* 2025). The present findings reinforce this concept by showing that square planting arrangements improved both structural and physiological canopy efficiency, enabling maize stands to better utilize higher plant densities without proportional yield penalties (Abuzar *et al.* 2011; Dubas 1988; Sulewska *et al.* 2013; Tharp and Kells 2001).

From a broader agronomic perspective, the present results can contribute to the understanding of spatial optimization as a practical tool for sustainable yield intensification (Lobell *et al.* 2009). Given increasing pressure on arable land resources and the growing demand for food, feed, and bioenergy, optimizing planting geometry may represent a relatively low-cost strategy for improving productivity without increasing external inputs (Lobell *et al.* 2009). Furthermore, integrating functional–structural plant modeling with field experimentation may facilitate the development of genotype-specific planting systems adapted to particular agroecological

conditions (He *et al*. 2021; Maddonni and Otegui 1996; Timlin *et al.* 2014). Under increasing climate variability, optimizing plant spatial arrangement may also become important for maintaining yield stability by improving light interception uniformity and reducing sensitivity to transient stress conditions such as drought or heat stress (Shen *et al.* 2020; Széles *et al.* 2023). As maize remains one of the most important cereal crops worldwide, these findings highlight the importance of integrating genotype × density × spatial arrangement interactions into future breeding and crop management strategies.

Conclusions

This study demonstrated that plant spatial arrangement and population density strongly influenced maize morphology, canopy structure, and yield by affecting intraspecific competition and resource-use efficiency. The square planting pattern outperformed the conventional rectangular arrangement by promoting more uniform canopy structure, improved light distribution, and more efficient resource utilization, resulting in higher yields, particularly at moderate plant densities. Grain yield increased up to approximately seven plants·m^{-2}, after which it declined due to intensified interplant competition. Certain hybrids performed better under high-density conditions, indicating the importance of canopy-efficient traits in maize breeding. From an agronomic perspective, integrating spatial uniformity with moderate plant density may represent a sustainable and low-input strategy for maize yield intensification. Future research should combine functional–structural plant modeling with field validation to develop genotype-specific spatial arrangements that optimize light interception, resource allocation, and yield performance across diverse environmental conditions.

References

Abate T., Shiferaw B., Menkir A., Wegary D., Kebede Y. 2015. Factors that transformed maize productivity in Ethiopia. Food Security 7: 965–981. DOI: https://doi.org/10.1007/s12571-015-0488-z

Abuzar M.R., Sadozai G.U., Baloch M.S., Shah I.H., Javaid T., Hussain N. 2011. Effect of plant population densities on yield of maize. Journal of Animal and Plant Sciences 21(4): 692–695.

Al-Naggar A.M.M., Atta M.M.M. 2017. Elevated plant density effects on performance and genetic parameters controlling maize (*Zea mays* L.) agronomic traits. Egyptian Journal of Plant Breeding 21: 227–241. DOI: https://doi.org/10.9734/JABB/2017/31550

Assefa Y., Carter P., Hinds M., Bhalla G., Schön R., Jeschke M., Paszkiewicz S., Smith S., Ciampitti I.A. 2018. Analysis of long-term study indicates both agronomic optimal plant density and increase maize yield per plant contributed to yield gain. Scientific Reports 8: 4937. DOI: https://doi.org/10.1038/s41598-018-23362-x

Azrai M., Zainuddin B., Syam'un E., Musa Y., Efendi R., Priyanto S.B., Andayani N.N., Aqil M. 2025. Canopy architectural and physiological traits for optimizing maize yield under high planting density. Frontiers in Sustainable Food Systems 9: 1469305. DOI: https://doi.org/10.3389/fsufs.2025.1469305

Badu-Apraku B., Fakorede M.A.B., Nelimor C., Osuman A.S., Bonkoungou T.O., Muhyideen O., Akinwale R.O. 2023. Recent advances in breeding maize for drought, heat and combined heat and drought stress tolerance in sub-Saharan Africa. CABI Reviews 2023: 1–22. DOI: https://doi.org/10.1079/cabireviews.2023.0011

Bereś P.K. 2012. Distribution of *Ostrinia nubilalis* Hbn. egg clusters on maize plants in south-eastern Poland in 2004–2008. Journal of Plant Protection Research 52: 106–113. DOI: https://doi.org/10.2478/v10045-012-0017-4

Çakir R. 2004. Effect of water stress at different development stages on vegetative and reproductive growth of corn. Field Crops Research 89: 1–16. DOI: https://doi.org/10.1016/j.fcr.2004.01.005

Duan M., Zhang X., Wei Z., Chen X., Zhang B. 2024. Effect of maize canopy structure on light interception and radiation use efficiency at different canopy layers. Agronomy 14: 1511. DOI: https://doi.org/10.3390/agronomy14071511

Dubas A. 1988. Obsada roślin a produktywność kukurydzy. W: Materiały konferencyjne „Obsada a produktywność roślin uprawnych". IUNG, Puławy: 112–120.

Erenstein O., Jaleta M., Sonder K., Mottaleb K., Prasanna B.M. 2022. Global maize production, consumption and trade: trends and R&D implications. Food Security 14: 1295–1319. DOI: https://doi.org/10.1007/s12571-022-01288-7

Feng L., Shi K., Liu X., Yang H., Pu T., Wu Y., Yong T. 2024. Optimizing trade-offs between light transmittance and intraspecific competition under varying crop layouts in a maize–soybean strip relay cropping system. Field Crops Research. DOI: https://doi.org/10.1016/j.cj.2024.10.010

Ghannoum O. 2009. C4 photosynthesis and water stress. Annals of Botany 103: 635–644. DOI: https://doi.org/10.1093/aob/mcn093

Greveniotis V., Zotis S., Sioki E., Ipsilandis C. 2019. Field population density effects on field yield and morphological characteristics of maize. Agriculture 9: 160. DOI: https://doi.org/10.3390/agriculture9080160

Haarhoff S.J., Swanepoel P.A. 2022. Plant population and row spacing affects growth and yield of rainfed maize in semi-arid environments. Frontiers in Plant Science 13: 761121. DOI: https://doi.org/10.3389/fpls.2022.761121

He L., Sun W., Chen X., Han L., Li J., Ma Y. 2021. Modeling maize canopy morphology in response to increased plant density. Frontiers in Plant Science 11: 533514. DOI: https://doi.org/10.3389/fpls.2020.533514

Kucharczyk H., Bereś P.K., Dąbrowski Z.T. 2011. Species composition and seasonal dynamics of thrips populations on maize (*Zea mays* L.) in south-eastern Poland. Journal of Plant Protection Research 51: 210–216. DOI: https://doi.org/10.2478/v10045-011-0036-6

Lai Z., Liao Z., Liu Y., Kou H., Li Z., Fan J. 2025. Optimized planting density and nitrogen rate improved grain yield of drip-fertigated maize by enhancing canopy structure and photosynthetic capacity. Journal of Agriculture and Food Research 21: 101813. DOI: https://doi.org/10.1016/j.jafr.2025.101813

Lashkari M., Madani H., Ardakani M.R., Golzardi F., Zargari K. 2011. Effect of plant density on yield and yield components of different corn (Zea mays L.) hybrids. Journal of Agricultural and Environmental Sciences 10: 450–457.

Li J., Xie R.Z., Wang K.R., Hou P., Ming B. 2018. Response of canopy structure, light interception and grain yield to plant density in maize. Journal of Agricultural Science 156: 303–315. DOI: https://doi.org/10.1017/S0021859618000692

Lobell D.B., Cassman K.G., Field C.B. 2009. Crop yield gaps: their importance, magnitude and causes. Annual Review of Environment and Resources 34: 179–204. DOI: https://doi.org/10.1146/annurev.environ.041008.093740

Maddonni G.A., Otegui M.E. 1996. Leaf area, light interception, and crop development in maize. Field Crops Research 48: 81–87. DOI: https://doi.org/10.1016/0378-4290(96)00019-7

Maddonni G.A., Otegui M.E., Cirilo A.G. 2001. Plant population density, row spacing and hybrid effects on maize canopy architecture and light attenuation. Field Crops Research 71: 183–193. DOI: https://doi.org/10.1016/S0378-4290(01)00158-7

Maddonni G.A., Otegui M.E. 2006. Intra-specific competition in maize: contribution of extreme plant hierarchies to grain yield and kernel composition. Field Crops Research 97: 155–166. DOI: https://doi.org/10.1016/j.fcr.2005.09.013

Maresma Á., Ballesta A., Santiveri F., Lloveras J. 2019. Sowing date affects maize development and yield in irrigated Mediterranean environments. Agriculture 9: 67. DOI: https://doi.org/10.3390/agriculture9030067

Martínez-Ortiz M.A., Salinas-Moreno Y. 2024. Challenges and opportunities in the specialization of maize cultivation. Agro Productividad 17(9): 81–92. DOI: https://doi.org/10.32854/agrop.v17i9.3037

Michalski T., Weber Z., Gołębniak B. 2000. Occurrence of diseases on triticale and barley plants grown in pure stands and their mixtures. Journal of Plant Protection Research 40: 198–204.

Moll R.H., Kamprath E.J. 1977. Effects of population density upon agronomic traits associated with genetic increases in yield of Zea mays L. Agronomy Journal 69: 81–84. DOI: https://doi.org/10.2134/agronj1977.00021962006900010021x

Page E.R., Tollenaar M., Lee E.A., Lukens L. 2010. Timing, effect, and recovery from intraspecific competition in maize. Agronomy Journal 102: 1007–1013. DOI: https://doi.org/10.2134/agronj2009.0397

Pelech E.A., Evers J.B., Pedersen T.L. 2023. Leaf, plant, to canopy: a mechanistic study on aboveground plasticity and plant density within a maize–soybean intercrop system for the Midwest USA. Plant Cell & Environment 46: 5123–5142. DOI: https://doi.org/10.1111/pce.14487

Ranum P., Peña-Rosas J.P., García-Casal M.N. 2014. Global maize production, utilization, and consumption. Annals of the New York Academy of Sciences 1312: 105–112. DOI: https://doi.org/10.1111/nyas.12396

Roth G.W. 1997. Potential of narrow corn production in Pennsylvania. Pennsylvania State University Agronomy Facts 52.

Sangoi L. 2001. Understanding plant density effects on maize growth and development: an important issue to maximize grain yield. Ciência Rural 31: 159–168. DOI: https://doi.org/10.1590/S0103-84782001000100027

Sangoi L., Gracietti M.A., Rampazzo C., Bianchetti P. 2002. Response of Brazilian maize hybrids from different eras to changes in plant density. Field Crops Research 79: 39–51. DOI: https://doi.org/10.1016/S0378-4290(02)00124-7

Shapiro S.S., Wilk M.B. 1965. An analysis of variance test for normality (complete samples). Biometrika 52: 591–611. DOI: https://doi.org/10.1093/biomet/52.3-4.591

Shen H., Chen Y., Wang Y., Xing X., Ma X. 2020. Evaluation of the potential effects of drought on summer maize yield in the Western Guanzhong Plain, China. Agronomy 10(8): 1095. DOI: https://doi.org/10.3390/agronomy10081095

Shiferaw B., Smale M., Braun H.J., Duveiller E., Reynolds M., Muricho G. (2013) Crops that feed the world 10: past successes and future challenges to the role played by wheat in global food security. Food Security 5: 291–317. DOI: https://doi.org/10.1007/s12571-013-0263-y

Song Y., Rui Y., Bedane G., Li J. 2016. Morphological characteristics of maize canopy development as affected by increased plant density. PLoS ONE 11: e0158610. DOI: https://doi.org/10.1371/journal.pone.0154084

Stewart D.W., Costa C., Dwyer L.M., Smith D.L. 2003. Canopy structure, light interception, and photosynthesis in maize. Agronomy Journal 95: 1465–1474. DOI: https://doi.org/10.2134/agronj2003.1465

Sulewska H., Koziara W., Śmiatacz K., Szymańska G., Panasiewicz K. 2013. Wpływ gęstości siewu na plonowanie odmian kukurydzy o różnej klasie wczesności. Nauka Przyroda Technologie 7(3): 1–10.

Széles A., Horváth É., Simon K., Zagyi P., Huzsvai L. 2023. Maize production under drought stress: nutrient supply, yield prediction. Plants 12(18): 3301. DOI: https://doi.org/10.3390/plants12183301

Szmigiel A., Oleksy A. 2004. Wpływ gęstości siewu na plon odmian kukurydzy o różnej klasie wczesności. Biuletyn Instytutu Hodowli i Aklimatyzacji Roślin 231: 437–444.

Szulc P., Jagła M., Nowosad K., Bocianowski J., Olejarski P. 2017. Path analysis in assessment of cause and effect dependencies of yield structure components in maize cultivars differing in genetic profiles. Fresenius Environmental Bulletin 26(12): 7309–7318.

Testa G., Reyneri A., Blandino M. 2016. Maize grain yield enhancement through high plant density cultivation with different inter-row and intra-row spacings. European Journal of Agronomy 72: 28–37. DOI: https://doi.org/10.1016/j.eja.2015.09.006

Tetio-Kagho F., Gardner F.P. 1988. Responses of maize to plant population density. II. Reproductive development, yield, and yield adjustments. Agronomy Journal 80: 935–940. DOI: https://doi.org/10.2134/agronj1988.00021962008000060019x

Timlin D.J., Fleisher D.H., Kemanian A.R., Reddy V.R. 2014. Plant density and leaf area index effects on the distribution of light transmittance to the soil surface in maize. Agronomy Journal 106: 1828–1837. DOI: https://doi.org/10.2134/agronj14.0160

Tharp B.E., Kells J.J. 2001. Effect of glufosinate-resistant corn (Zea mays) population and row spacing on light interception, corn yield, and common lambsquarters growth. Weed Technology 15: 413–418. DOI: https://doi.org/10.1614/0890-037X(2001)015[0413:EOGRCZ]2.0.CO;2

Toler J.E., Murdock E.C., Stapleton G.S. 1999. Corn leaf orientation effects on light interception, intraspecific competition, and grain yields. Journal of Production Agriculture 12: 100–104. DOI: https://doi.org/10.2134/jpa1999.0396

Wang Q., Sun Z., Bai W., Zhang D. 2021. Light interception and use efficiency differ with maize plant density in maize–peanut intercropping. Frontiers of Agricultural Science and Engineering 8: 591–604. DOI: https://doi.org/10.15302/J-FASE-2021403

Voldeng H.D., Bloukman G.E. 1975. Interaction between genotype and density on the yield components of Zea mays. II. Grain production. Journal of Agricultural Science 84(1): 61–74. DOI: https://doi.org/10.1017/S0021859600052088

Yan J., Warburton M., Crouch J. 2011. Association mapping for enhancing maize (*Zea mays* L.) genetic improvement. Crop Science 51: 433–449. DOI: https://doi.org/10.2135/cropsci2010.04.0233

Zhai L., Zhang L., Yao H., Zheng M., Ming B., Xie R. 2022. Optimal cultivar × sowing date × plant density for grain yield and resource use efficiency of summer maize in China. Agriculture 12: 7. DOI: https://doi.org/10.3390/agriculture12010007

Zhao L., Duan X., Zhang X., Zhang X., Song L., Chen P., Liang M., Zhang C., Wang C. 2025. Planting strategy optimization can increase maize yield by delaying leaf senescence and improving photosynthetic capacity. Agronomy 15: 1099. DOI: https://doi.org/10.3390/agronomy15051099

Table 7. ANOVA test for tested traits

Source of variation Trait	d.f.	EL	KBL	ED	H1	H2	PC	FC	SC	TKW	LAI	Y
FacII	1	0.818	0.546	0.00656	18.6	4.5	0.0025	0.01778	0.0011	61.8	3.3215	0.024
Residual	2	1.448	4.993	0.011061	479	518.3	0.8406	0.01403	1.7389	320.6	0.2172	0.965
FacI	1	63.736**	19.175	2.252977**	274.5	128.5	10.3469*	3.36111*	74.2469**	130366.7**	3.6259*	55.5522*
FacI.FacII	1	0.854	8.513	0.04405	660.5	817.6	0.4225	0.00694	0.0069	129	0.7966	0.3211
Residual	2	0.111	1.398	0.006494	297.2	58.2	0.4544	0.05403	0.2369	1155	0.1516	1.0507
FacIII	2	1.477	3.805	0.004878	50.5	27.6	0.3097	0.0034	0.084	123.1	0.1467	10.1543
FacI.FacIII	2	0.412	0.316	0.009013	81.5	118.6	0.0834	0.0409	0.6751	306.4	0.0811	0.153
FacII.FacIII	2	15.874	32.381	0.067671	6.6	88.1	3.0202	0.07799	1.4947	1412.8	0.0218	20.7339
FacI.FacII.FacIII	2	0.97	0.343	0.021322	6.3	72.5	0.6015	0.00132	0.253	221.4	0.3148	3.4799
Residual	8	13.035	21.397	0.038594	135.4	283.1	2.0769	0.03965	1.0654	464.4	0.2678	26.6722
Year	2	24.871***	6.731**	0.042513*	47013.1***	59516***	44.8551***	13.3609***	3348.1069***	15767.8***	46.6348***	11.3494***
Year.FacI	2	27.709***	14.359***	0.176215***	3126.5***	4572.1***	2.3951***	0.09215**	27.9488***	1243.9*	9.6219***	0.7619
Year.FacII	2	0.146	0.377	0.00173	429.5	109.4	0.5052	0.00465	0.0659	193.1	4.3116***	0.2494
Year.FacIII	4	1.307	1.128	0.001273	128.5	143	0.2928	0.02757	0.1746	261.4	0.9586	1.5437
Year.FacI.FacII	2	2.077	5.028*	0.006951	1141.9**	196.2	1.2119*	0.00424	1.3259*	378	3.3932**	4.1479**
Year.FacI.FacIII	4	0.853	0.977	0.00903	54.2	127.7	0.074	0.01507	0.3769	63.4	0.9271	1.0709
Year.FacII.FacIII	4	1.63	0.311	0.002291	349	168.8	0.2317	0.02111	0.0944	277.7	0.1934	0.7376
Year.FacI.FacII.FacIII	4	1.55	0.252	0.007233	34	217.4	0.2221	0.01486	0.1894	16	1.8316	0.6415
Residual	96	1.421	1.258	0.009033	193.4	157.8	0.3018	0.01543	0.3268	338.5	0.512	0.65

Fac I –factor I maize cultivar; Fac II– factor 2 spatial arrangement (rectangular, square); Fac III– factor III number of plants·m^{-2}; EL–ear length; KBL–kernel-bearing ear length; ED–ear diameter; H1–plant height at the 1st observation; H2–plant height at the 2nd observation; PC–protein content FC–fat content; SCs–starch content; TKW–thousand kernel weight; LAI–leaf area index; Y–yield; d.f.– degrees of freedom

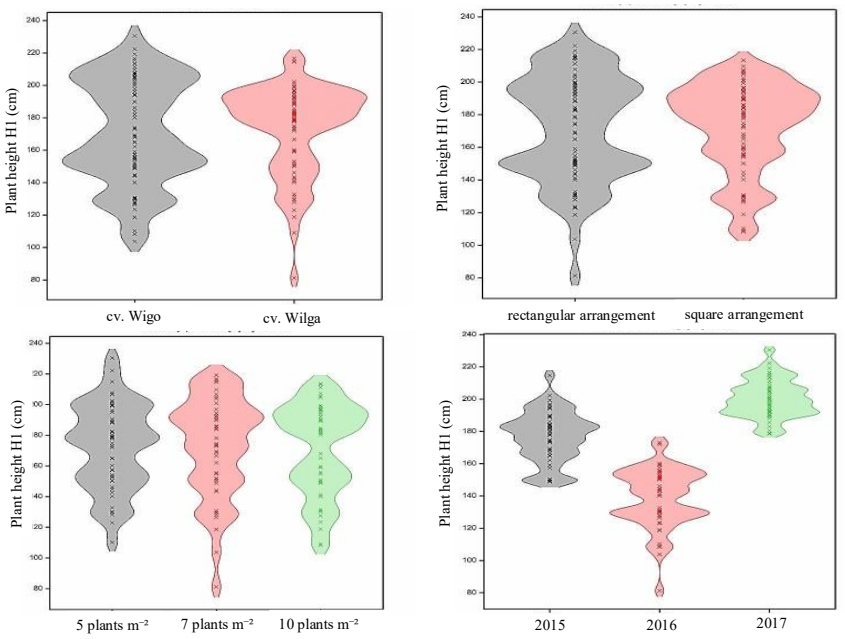

Fig. 2. Density plot of maize height at the first term of observation (H1) depending on the cultivar, spatial arrangement, sowing density and year

	EL	KBL	ED	H1	H2	PC	FT	SC	TKW	LAI	Y
EL	-										
KBL	0.8355	-									
ED	0.44	0.4667	-								
H1	0.2636	0.2465	-0.0704	-							
H2	0.1148	0.0825	0.0749	0.8343	-						
PC	0.3248	0.3691	-0.1058	0.5766	0.4573	-					
FT	0.3567	0.2484	0.3145	0.674	0.7916	0.4781	-				
SC	-0.1952	-0.1128	-0.1059	-0.755	-0.8728	-0.5544	-0.9286	-			
TKW	0.3723	0.305	0.6816	-0.5285	-0.4436	-0.4809	-0.1299	0.4003	-		
LAI	0.2004	0.1571	0.3473	0.4833	0.638	0.345	0.6483	-0.6284	-0.1545	-	
Y	-0.0899	-0.2698	0.0403	0.1349	0.1456	-0.2687	0.205	-0.1693	0.1422	0.0913	-
	P<0.05	P<0.01	P<0.001								

EL− ear length; KBL−kernel-bearing ear length; ED−ear diameter; H1−plant height (1st observation); H2−plant height (2nd observation); PC−protein content; FC−fat content; SC−starch content; TKW−thousand kernel weight; LAI−leaf area index; Y−yield

Fig. 3. Heat map of the interdependence of the observed features for 3 years study

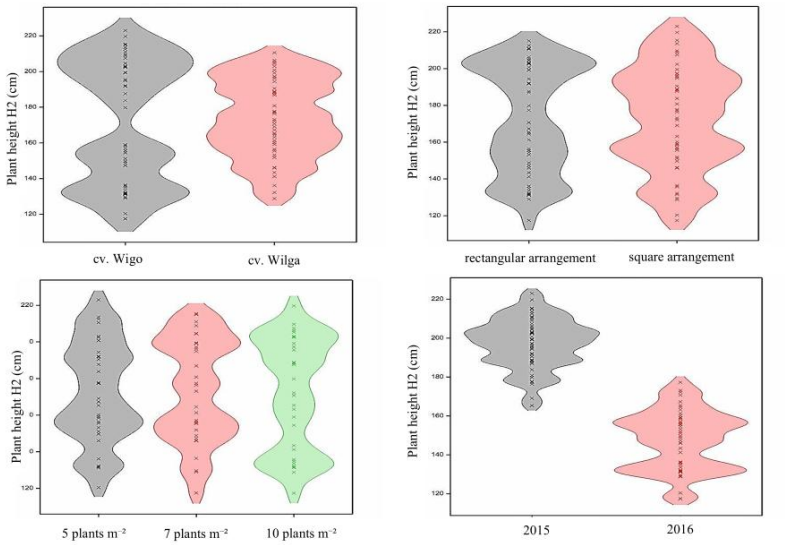

Fig. 4. Density plot of maize height at the second term of observation (H2) depending on the cultivar, spatial arrangement, sowing density and year

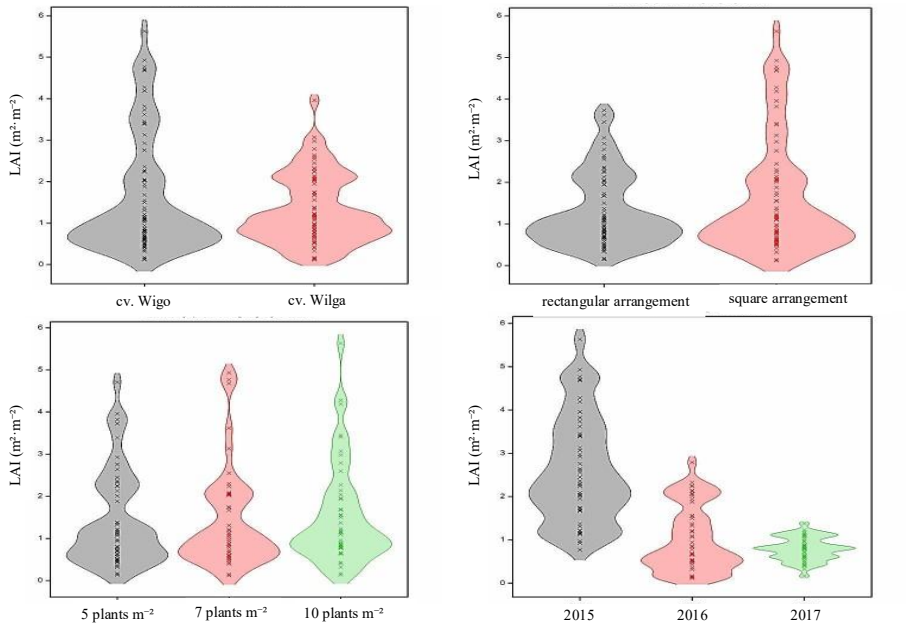

Fig. 5. Density plot of leaf area index (LAI) depending on the cultivar, spatial arrangement, sowing density and year

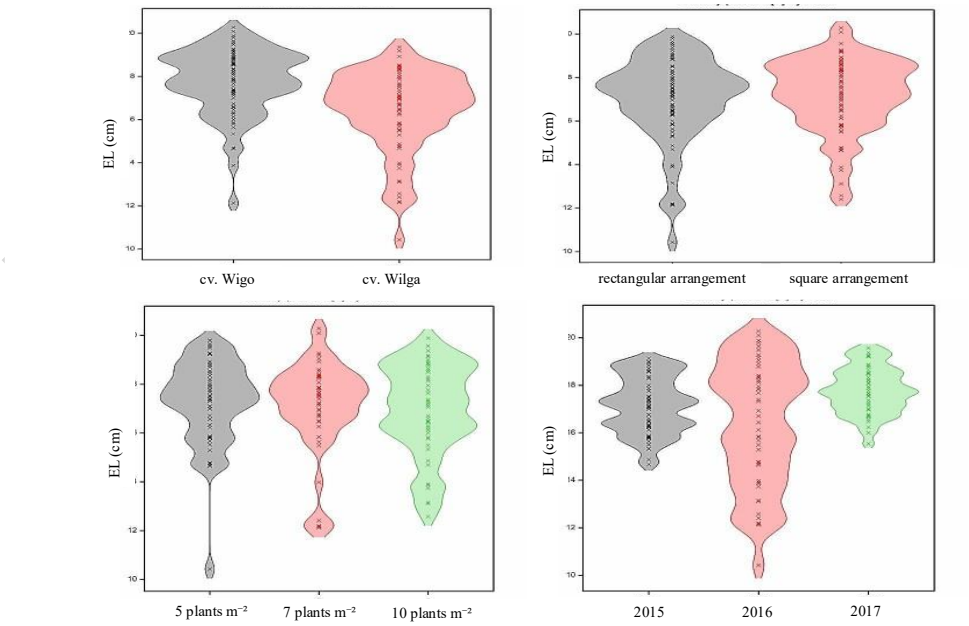

Fig. 6. Density plot of the ear length (EL) depending on the cultivar, spatial pattern, sowing density and year

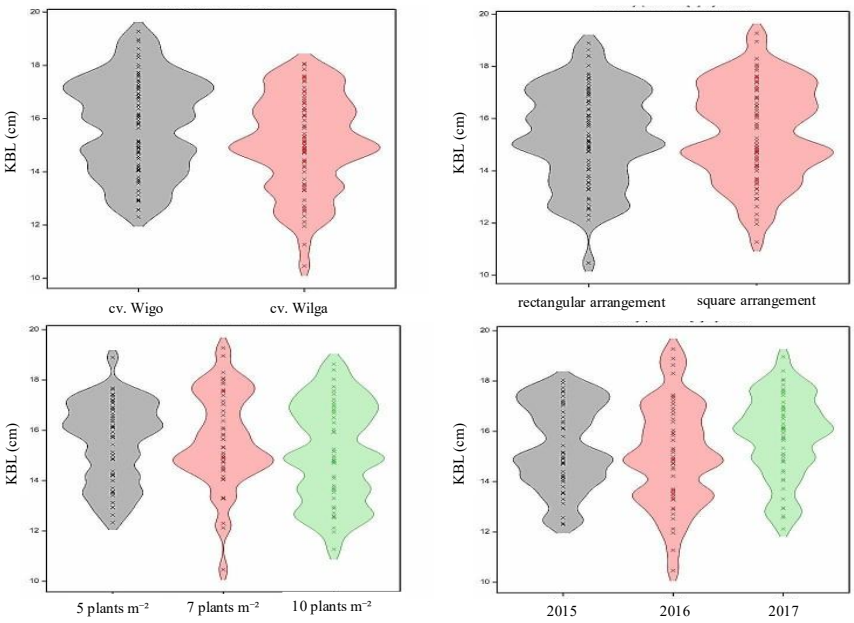

Fig. 7. Density plot of kernel-bearing ear length (KBL) depending on the cultivar, spatial pattern, sowing density and year

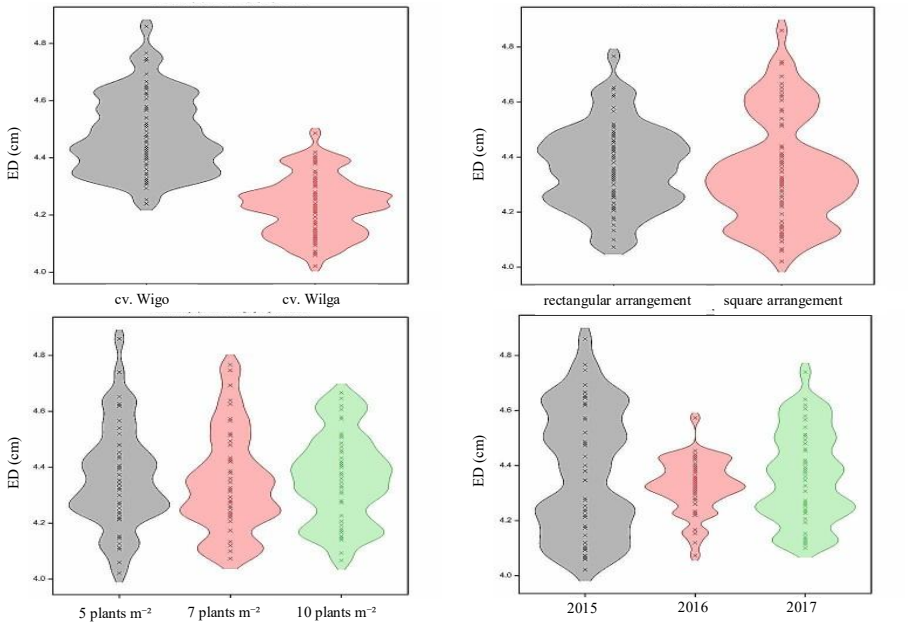

48

49 **Fig. 8.** Density plot of maize ear diameter (ED) depending on the cultivar, spatial pattern, sowing
50 density and year

51

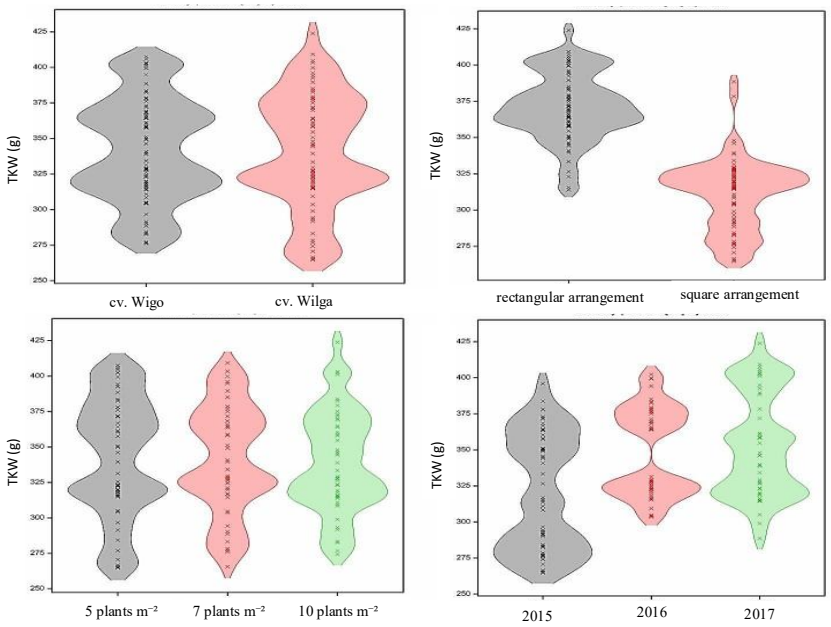

Fig. 9. Density plot of thousand kernel weight (TKW) depending on cultivar, spatial pattern, sowing density and year

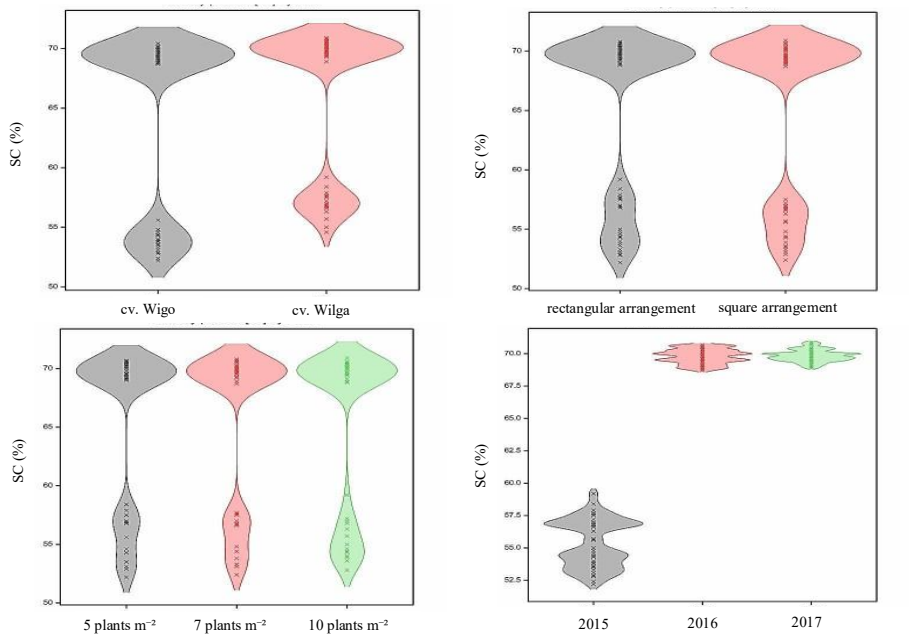

Fig. 10. Density plot of grain starch content (SC) depending on the cultivar, spatial pattern, sowing density and year

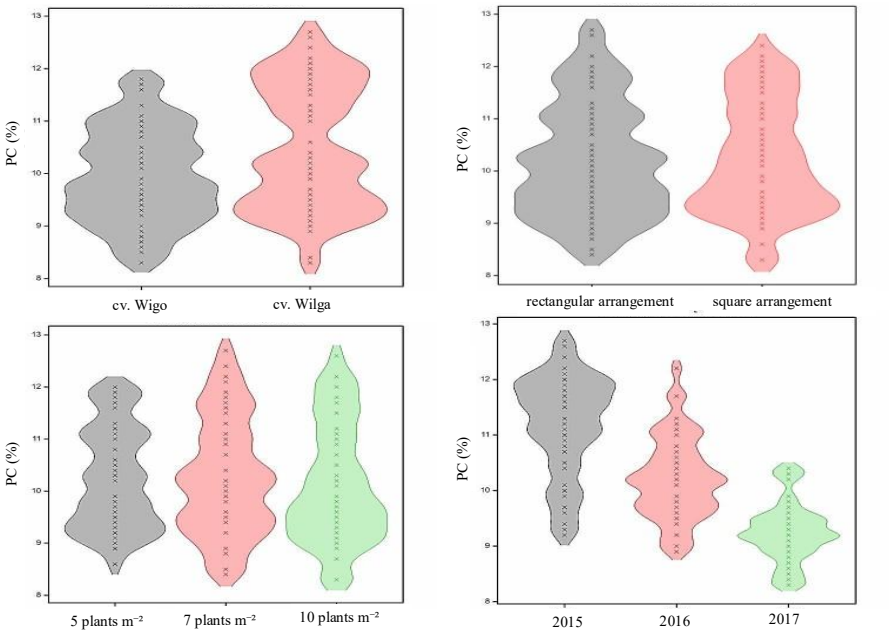

Fig. 11. Density plot of grain protein content (PC) depending on the cultivar, spatial pattern, sowing density and year

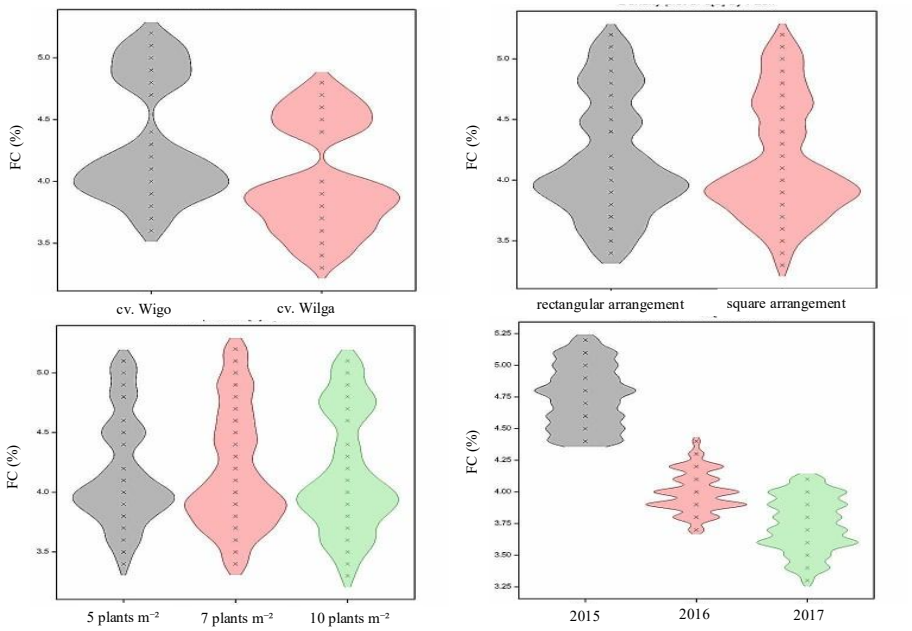

Fig. 12. Density plot of grain fat content (FC) depending on the cultivar, spatial pattern, sowing density and year

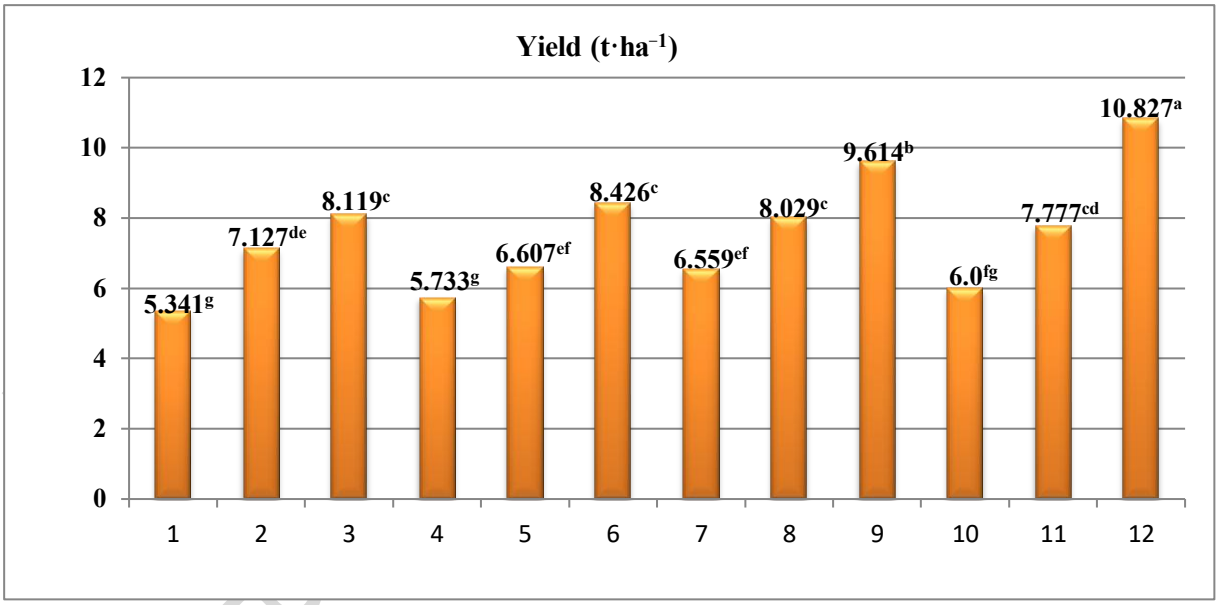

1. cv. Wilga; 100x20; 5 plants·m^{-2}; 2. cv. Wilga; 37.8x37.8; 7 plants·m^{-2}; 3. cv. Wilga; 70x13.6; 10.5 plants·m^{-2}; 4. cv. Wilga; 44.7x44.7; 5 plants·m^{-2}; 5. cv. Wilga; 85x16.8; 7 plants·m^{-2}; 6. cv. Wilga; 30.9x30.9; 10.5 plants·m^{-2}; 7. cv. Wigo; 100x20; 5 plants·m^{-2}; 8. cv. Wigo; 37.8x37.8; 7 plants·m^{-2}; 9. cv. Wigo; 70x13.6; 10.5 plants·m^{-2}; 10. cv. Wigo; 44.7x44.7; 5 plants·m^{-2}; 11. cv. Wigo 85x16.8 7 plants·m^{-2}; 12. cv. Wigo; 30.9x30.9; 10.5 plants·m^{-2}

Fig. 13. Average grain yield of maize in the years 2015–2017

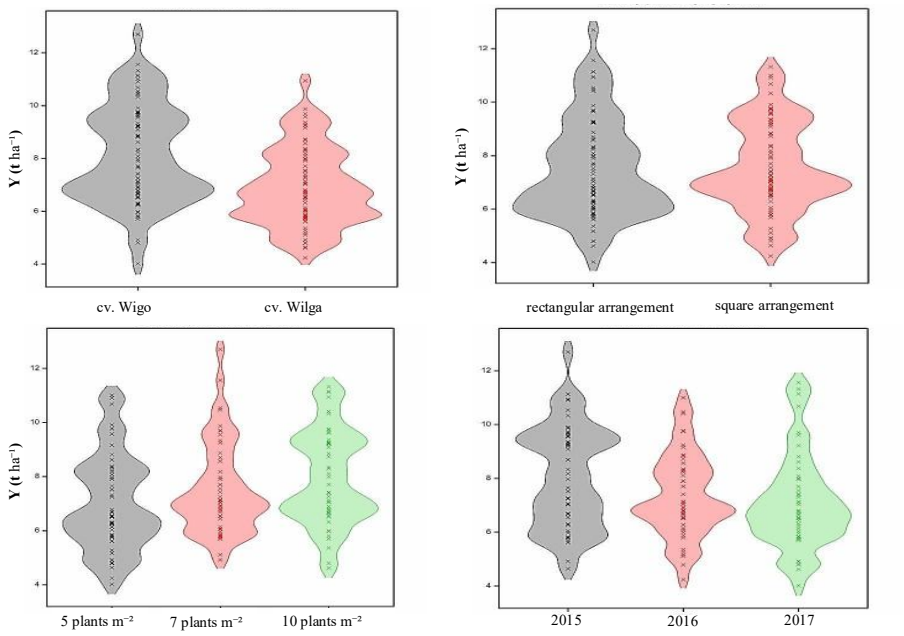

Fig. 14. Density plot of yield (Y) depending on the cultivar, spatial pattern, sowing density and year